Wind Speed Influences Corrected ~~Auto-calibrated~~Autocalibrated Soil Evapo-respiration Chamber (ASERC~~),)~~ Evaporation Measures.

Bartosz M. Zawilski

CESBIO Université de Toulouse, CNES, CNRS, INRA, IRD, UPS, Toulouse, 31000 France

Correspondence to: Bartosz M. Zawilski (zawilskib@cesbio.cnes.fr)

Abstract. ~~The importance of the~~ Soil evaporation concerns water, and our ~~main~~ life supports ~~source~~sources that are important for agriculture or for climate ~~changes predictions~~change prediction science. A simple ~~to operate~~ instrument~~,~~ based on ~~non-steady~~the nonsteady state (NSS) technique~~, made~~ for soil evaporation measurement appears ~~then~~ suitable. However, because the NSS chamber technique is highly invasive, special care should be provided to correct the wind speed influence on the evaporation process. ~~As the wind influence on the~~ Soil evaporation is ~~depending~~a complex process that involves many soil and air characteristics. Measurement chamber installation on the soil and its head deployment may perturb these characteristics. We then had to minimize differences or to correct the measurements. Most of the differences between bare soil and soil with a deployed chamber head can be minimized except for the wind speed influences that are not reproductible inside a chamber head. Meanwhile, as the wind influences depend on numerous and not real-time monitorable variables, ~~in order~~ to make the measurements easily corrigible on ~~a~~ bare soil with a unique variable~~–~~, wind speed (*Ws*), ~~whatever is~~regardless of the soil ~~nature~~composition, soil texture, and ~~others~~other soil or air meteorological variables~~—~~, a self-calibrating chamber with a corresponding protocol called ~~Auto-calibrated~~the Autocalibrated Soil ~~Evapo-Respiration~~Evaporespiration Chamber (ASERC) was developed. A simple protocol followed by this chamber allows us to determine the soil evaporation wind speed susceptibility (Z) and to correct the measurements achieving 0.95 ~~accuracy confidence.~~as the coefficient of determination. Some interesting ~~finding~~findings on sandy and clayey ~~soils~~soil evaporation measured during ~~a~~ laboratory calibration and "slow" sensor simulation will also be reported in the two appendices.

Frequently used acronyms and units if applicable.

AEV: Air Entry Value

ASERC: Auto-calibrated Soil Evapo-Respiration Chamber

CAEV: Cracking Air Entry Value

CP: Common Point

ER: Exponential Rise

IR: Infra-Red

IRGA: Infra-Red Gas Analyzer

$m(W_S)$: correction factor depending on wind speed.

M: Measurement average multiplied by Z ($gm^{-2}s^{-1}$)

M_x: Measurement with PWM=x% ($gm^{-2}s^{-1}$)

$M_{10\text{-}30}$: Average of the measurement with PWM=10% and measurement with PWM=30%

M_B : bucked with soil mass (g)

M_0: bucket with dry soil mas (g)

M_s: dry soil mass (g)

MAEV: Matrix Air Entry Value

ME: Measured Evaporation ($gm^{-2}s^{-1}$)

NDIR: Non-Dispersive Infra-Red

NSS: non-steady state

P: Water vapor Production ($gm^{-2}s^{-1}$)

PTFE: Polytetrafluoroethylene

PU: polyurethane

PWM: Pulse Wide Modulation (unitless and expressed in %)

q: Absolute air humidity (gm^{-3})

R^2: coefficient of determination

RE: Real Evaporation ($gm^{-2}s^{-1}$)

RH: relative air moisture (unitless but expressed in %)

S: Soil water vapor Stock (gm^{-2})

SWC: Soil Water Content

Ta: Air temperature (°C)

τ_{63}: Response Time (time necessary to reach 63% of final signal) (s)

W: Gravimetric soil water content (unitless expressed in %)

Ws: Wind speed (m/s)

Z: soil evaporation wind susceptibility (unitless and expressed in %)

$Z_{10\text{-}30}$: Z calculated using only two measurements with PWM=10% and PWM=30%

Z_{total}: Z calculated using all ten measurements with PWM from 10 to 100% (step 10%).

Introduction. In the context of rising global temperature ~~rising~~, as ~~the~~ water is our main life support key resource ~~to the~~for food production, and ~~the~~ water vapor is one of the most abundant greenhouse gases in the ~~Earth~~Earth's atmosphere, it is important to gather knowledge about soil evaporation. Soil evaporation may be a major soil moisture loss source. On the one

hand, the global direct ~~annual~~ soil evaporative ~~precipitations lose~~annual precipitation losses are as high as 20~~%~~%, and the other 40% ~~though the~~of precipitation losses are due to vegetation transpiration (Oki and Kanae 2006~~),~~). In arid and ~~the~~semiarid regions, soil evaporation may reach up to 75% ~~in the arid and semi-arid regions (WMO168-2008~~of the precipitation (Riou, 1997) when ~~the~~ total soil evaporation along with ~~the~~ vegetation transpiration, so-called evapotranspiration, may dissipate up to 90% of the annual ~~rain-fall~~precipitation (Pilgrim et ~~all~~al., 1988~~,~~; Wilcox et ~~all.~~al., 2003). On the other hand, ~~the~~ soil evaporation consumes ~~about~~approximately 20% of ~~the~~ solar radiation energy (Trenberth et al~~.~~., 2006). Energy absorbed on the soil surface or in the soil subsurface during the evaporation process, lowering ~~down~~ soil temperature, is released later in the higher atmosphere layer when condensing, warming up the air. ~~The~~ Water vapor is the most important greenhouse gas in the atmosphere not because of its efficiency but because it is the most ~~present~~abundant; 60% of the total greenhouse effect (Trenberth et al~~.~~., 2009, Schmidt et ~~all.~~al., 2010) and its recently measured upper-tropospheric concentration increase ~~is~~are directly attributable to ~~the human's~~human activities (Choung et al. 2014). Good et al. (2015) ~~shows~~showed that the main water vapor source (65%) ~~is~~was the soil ~~and not~~ surface ~~waters. Motivated especially by measured soil energy budget imbalance of a notable importance and a probable subsurface evaporation contribution, a simple and versatile soil evaporation measurement instrument was developed based on a Non-Steady-State (NSS) automatic chamber technique, with special attention given to the solar radiation heating screening and the wind influence corrections. Chamber construction and it characteristic such as real mixing time assessment, developed protocol for evaporation calculations, and wind influence corrections will be reported. This study is based on over 1000 measurement cycles (that is over 10 000 chamber deployments during over two years) and, after calibration of wind influence on the evaporation and chamber perturbations correction, showing a reasonable agreement between chamber measurements and real evaporation with $R^2 > 0.95$. The same correction formula is used for sandy and clayey soils whatever is the soil moisture~~, not the water surface.

~~1 Existing evaporation measurement~~ Water vapor effluxes are commonly measured using different techniques. The widely used eddy covariance technique is a relatively expensive but ~~little~~minimally invasive way to estimate ~~the~~ soil evaporation on ~~the~~ bare soil and other trace ~~gases~~gas fluxes. ~~As~~This technique consists of a high-frequency air analysis, typically by a nondispersive infrared (NDIR) or infrared gas analyzer (IRGA) at 10 or 20 Hz along with a high-frequency air velocity measurement by an ultrasonic anemometer. From these measurements, a covariance is deduced that allows us to compute the trace gas fluxes. As with every measurement technique, eddy covariance has its ~~pro~~pros and cons. Eddy covariance provides ~~the~~ evaporation estimation when the air flow is turbulent enough ~~that~~, which means only when the wind is strong enough, which is usually not the case at night. ~~Also~~Additionally, these measurements are not precisely localized, and the provenance is approximative. This point is often a force since the measurements ~~reflecting~~reflect the mean process but not when a precise provenance is sought -after. However, eddy covariance cannot be implemented everywhere. The site should be flat and big enough~~,~~ (please see the book edited by Aubinet et al. (2012~~)~~), an eddy covariance -dedicated book which ~~is describing~~describes this technique and its requirements from a practical point of view~~. Also~~). Additionally, a systemic underestimation of eddy covariance CO_2 flux ~~comparatively~~compared to closed ~~chambers techniques given~~ chamber technique measured fluxes was pointed out by ~~numerus~~numerous authors (Goulden et al~~.~~., 1996~~,~~; Norman et al~~.~~., 1997~~,~~; Law et al~~.~~., 1999~~,~~; Hollinger et al~~.~~.,

1999;; Janssens et al.., 2000;; Pavelka et al.., 2007;; Zha et al.., 2007;; Myklebust et al.., 2008;; Schrier-Uijl et al.., 2010). Nevertheless, we have to keptmust keep in mind that chamberschamber measurements have to be carefully considered and, in the same way as for evaporation, other gasesgas efflux measurements have to be corrected versus the wind (Zawilski in progress). In the speed. Under calm conditions, due to the internal fan perturbations, closed chambers may have a tendency to overestimate a possible soil efflux (Schneider et al.., 2009;; Brændholt et al.., 2017).

In the case of the presence of vegetation presence, in order, to separate transpiration from soil evaporation, an experimental isotopic mass balance approach can be adopted (Ferretti et al.., 2003) which). This technique requires a frequent soilair sampling and laboratory analyzeanalysis or expensive and voluminous analyzer use. Eddy covariance measurements giving agive total (soil evaporation and vegetation transpiration) evapotranspiration. Coupled with a partitioning accordinglyaccording to a model (see Koola et al. (2014) for a review) are performed to separate), a separation of soil and vegetation contribution.contributions is possible. Each specific model may be accurate but only for a specific plant, making it difficult to apply itthe model to a mixed plant cover. Moreover, even for a specific plant, there are numerous models giving different results. Nothing that for theFor maize, there are over 29 models (Kimball et al.., 2019). AlsoAdditionally, each model requires more or less numerous variable injections, which make some models difficult to be appliedapply since the required variables are not known (Kustas and Agam, 2014).

Another widely used technique for direct soil evaporation measurements is the lysimeters from a micro-lysimetersmicrolysimeters for bare soil evaporation measurementmeasurements to a large-scale lysimeters in order to measure the total evapotranspiration (listed by Liu et allal. 2002.). This technique consists roughly in weighting of weighing a hold soil colon, giving a direct evaporation or evapotranspiration measurement if the surface of the soil colon is large enough to hold supplementary vegetation. However, this apparatus should be buried deeply buried, making this measurement relatively hard to implement this measurement , especially when frequent apparatus displacements are necessary, as it is the case on an agricultural plot (tillage and others soilsother soil operations). Lysimeters also require also a deep enough soil, which is not the case with the presence of shallow rock presence and even simple stones presence, and provide a timely averaged measurement because the weighweight variation caused by water evaporation needs to be important enough comparativelycompared to the total enclosed soil weighweight.

Relatively recently, a heat balance-based method using the heat pulespulse probes was proposed by Sauer et al. (2007) and Heitman et al. (2008 and 2017). This technique is based on assumptionassumes that the heat budget disclosure is due only due to the water evaporation and allows measurements only in the subsurface, leaving the surface evaporation unmeasurable. YetHowever, this technique is the only one which technique that allows tracking the depths of theus to track subsurface evaporation with depth.

Therefore, an exclusive, fast and easy-to-implement total bare soil evaporation measurement is suitable. A dynamic closed Non-Steadynonsteady state (NSS) technique, used for soil effluxestrace gas efflux measurements may be also be used for soil evaporation assessment. However, for these measurements as, probably more than for other soil effluxesefflux measurements, measured data have tomust be carefully corrected. Indeed, this technique is not a direct measurement and is highly invasive.

Not only may the collar inserted into the soil ~~may~~ perturb the comportment of the enclosed soil by root shearing (Heinemeyer et al.~~.~~, 2011~~)~~), thereby limiting the autotrophic component of the respiration, but ~~also just by~~ the chamber presence and also more particularly during the chamber head deployment with the enclosed part of the soil isolation from the exterior meteorological conditions such as the wind perturbs the comportment of the enclosed soil (see Rochette et al.~~.~~, 1997 ~~and~~; Rochette and Hutchinson, 2005 for chamber technique description). Notably, motivated by the measurement of the soil surface energy budget imbalance and a probable subsurface evaporation contribution, a simple and versatile soil evaporation measurement instrument was developed. Based on an automatic nonsteady state (NSS) chamber technique, special attention is given to solar radiation heating, pressure variation preservation and wind speed influence. Chamber construction and its characteristics, the developed protocol for evaporation calculations and the developed calculation algorithms are reported. Wind speed influence is different on sandy and clayey soil, which could be explained by bay soil water vapor sorption and will be discussed along with unexpected inertia behavior. The latter phenomena require some precautions but allow us to assess the chamber head air mixing time. Finally, the wind speed influence correction function is presented.

This study is based on over 1000 measurement cycles (that is, over 10 000 chamber deployments over two years) and, after calibration of the wind speed influence on the evaporation and chamber perturbation correction, shows reasonable agreement between chamber measurements and real evaporation with $R^2 > 0.95$. The same correction formula is used for sandy and clayey soils regardless of the soil moisture.

1 Wind influence considerations

The wind influence on soil water vapor efflux is well known and widely studied (Thornthwaite and Holzman, 1942; Hanks and Woodruff, 1958). Even if a nondiffusive regime for a soil evaporation process were explored more than a half century ago (Fukuda, 1955), considering a gusty wind influence from the theoretical point of view by a sinusoidal representation, concluding with a negligibility of the phenomenon, other authors studied and experimented with wind-influenced evaporation (Farrell et al., 1966; Scotter and Raats, 1968) and concluded, on the contrary, that a nondiffusive regime had great importance. Recently, numerous authors experimentally and theoretically studying gas propagation in porous media have pointed out an important or even the largest role of nondiffusive regimes, such as thermal and solutal dispersion (Davarzani et al., 2014), convection and advection or pressure fluctuations for gas movement through porous media (soil); see Sánchez-Cañete et al. (2016) and the references given there. One of the major gas movement causes is *wind pumping*, which includes three effects:

- The Venturi effect (Xu et al., 2005; Bain et al., 2005; Suleau et al., 2009) gives rise to mass transfer by establishing a pressure gradient.
- Natural gradient concentration disturbances (Le Dantec et al., 1999; Longdoz et al., 2000; Lai et al., 2012) play an important role during very calm conditions, and a highly stratified boundary layer slows the diffusion efflux and, once disturbed by the head space mixing fan, releases an unusual high apparent efflux.
- Eddy pressure fluctuations cause gas dispersion (Maier et al., 2010; Mohr et al., 2016; Brændholt et al., 2017; Pourbakhtiar et al., 2017; Poulsen et al., 2017; Mohr et al., 2017), which may be a very important gas transport regime.

This effect is more or less screened by chamber deployment, depending mainly on the wind importance versus the internal head air mixing fan disturbances.

-

All these effects may be altered by a deployed chamber head and then affect the closed chamber measurements versus natural soil efflux. As the wind cannot be reproduced inside the chamber heads, the only possibility is to minimize the differences and to correct the data by calibrating the measurements versus the wind speed, which is the aim of this paper in presenting an adapted nonsteady state dynamic chamber technique and wind speed corrected for the water vapor efflux measurement.

The wind characteristics, such as friction velocity, have a very important influence on evaporation, contributing to evaporating water vapor from the boundary layer and maintaining a low ambient air humidity (Monin-Obukhov similarity theory, see, for example, Hill, 1989). Then, as the water demand is still high (water vapor demand) is complementary to relative humidity (*RH*), water vapor production is consequent. If the air humidity is high, with or without important friction velocity, the soil evaporation is low. Turbulence (quantified by friction velocity) has a great influence on air humidity (quantified by water vapor demand), which has a great influence on soil evaporation. As described in further sections of this paper, the chamber operation protocol is optimized for initial air humidity preservation, preserving the initial water vapor demand. Consequently, one can reasonably assume that the chamber measurements do not have to be corrected versus the air water vapor transport ability (friction velocity).

Another consequence of the presence of turbulence is pressure oscillations. As the chamber head includes an expansion room equalizing pressures between the deployed chamber head internal volume and the exterior pressure, there is no special correction to perform for the pressure fluctuations.

The only pertinent wind characteristic that appears to be important but not preserved is the wind speed.

2 Materials and methods

2.1 Chamber construction

The chamber described later in this paper was constructed in the laboratory (please see Fig. 01).

~~**2 Materials and methods**~~

~~**2.1 Chamber construction**~~

~~The chamber described later in this paper was constructed in the laboratory (please see Fig. 01).~~

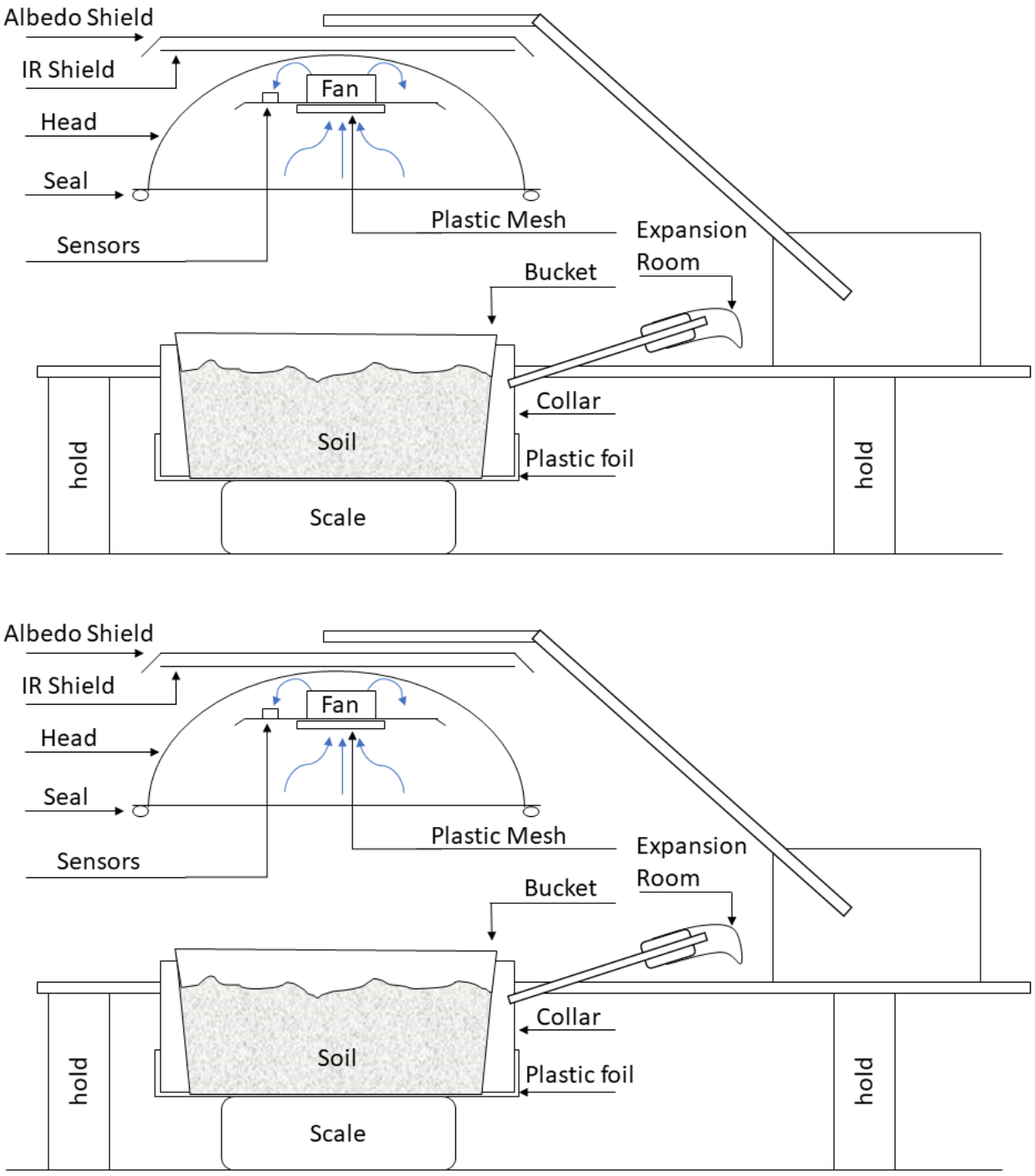

Figure 01: Scheme of the chamber and experimental setup. In this sketch, the chamber head is not deployed.

When the chamber head is deployed, the cloche with embedded fan is firmly put down on the base insulating the collar with the bucket and a well delimited air ~~portion~~volume. Inside this finite air volume, due to ~~the~~ soil evaporation, the relative air moisture *RH* will rise more or less quickly up to ~~reach 100%.~~the saturation value, which is important depending on the soil matrix suction.

~~Used~~The internal fan, which is the core of the device, is a Maglev fan PSD1204 PKB 3-A ~~40x40x20mm~~40 mmx40 mmx20 mm (Sunonwealth Electric Machine Industry Company Limited, Qianzhen, District Kaohsiung, Taiwan) with pulse ~~Wide~~width modulation (PWM) control and rotation sensor driven by a generic PWM generator able to generate a signal of a given frequency and a given duty on demand ~~and,~~ communicating with a datalogger (CR1000 from Campbell Scientific, Logan, ~~Utah~~UT, USA~~.))~~ by a UART ~~(~~TTL~~)~~ bus. The main humidity sensor (because there were three ~~of~~ humidity sensors of ~~a~~ different response time for comparison) is a P14 Rapid mounted on a Linpicco plate with a PT1000 sensor for simultaneous humidity and temperature measurements (Innovative Sensor Technology IST AG, Ebnat-Kappel, Switzerland). ~~A~~The pressure, temperature and ~~also~~ humidity ~~again~~ inside the chamber head were monitored using a BME280 (Bosch Sensortec GmbH, Reutlingen, Germany) ~~a~~ digital sensor under an Arduino-Uno control (I²C bus) forwarding these measures to the main data logger CR1000 via UART, TTL bus. The fan, mounted on a holding plate along with all the sensors, ~~was aspirating~~aspirated the air from the bottom of the chamber head through a plastic mesh (opening percentage 47%). ~~Not~~The digital scale used ~~for this paper but for respiration measurements, an embedded carbon dioxide sensor MH-Z16 (Winsen Electronics Technology~~was a WA30002Y from W&J Instrument Co~~.~~., Ltd~~, Zhengzhou, Henan.~~, Mudu Jiangsu, China~~) based on a Non-Dispersive Infra-Red (NDIR) technique,~~ with a ~~digital interface (UART TTL) under an Arduino-Uno control~~continuous RS-232 bus output and 0.01 g resolution.

~~=~~The NSS ~~All internal metallic parts were coated with a high PTFE (Teflon) content paint in order to reduce as much as possible the water vapor sorption on a metallic surface.~~

~~Inside the collar was inserted a small pipe allowing the air entrapped by the chamber head, during the chamber deployment, flow freely through to inside a nitrile finger cot (expansion room) in order to equilibrate the inside and outside pressure and allowing a small chamber volume expansion to compensate the mass flow from the soil.~~

~~As the heating from solar radiations may strongly affect the evaporation process by artificially rising the chamber head temperature, a special attention was given to shield it with a first albedo shield made from a white painted stainless steel plate. This shield is screening direct radiations however its temperature will rise and its infra-red radiations may reach the chamber head as well. A well known~~ technique ~~used~~ has been known for ~~a cryogenics fluids operation was then used by interposing a second Infra-Red (IR) shield made from a plastic plate coated with an aluminium thick foil on both sides.~~

All calculations were automatized using a LabView 2015 programming (National Instruments Corporation, Austin, Texas USA)

2.2 Measurements protocol

For all the calibration measurements, the chamber was placed on holds and the collar bottom, normally inserted into the soil, was hatched with an elastic plastic foil. An electronic scale was placed just below this foil and a bucket with a studied soil was placed inside the collar reposing on the scale (digital scale WA30002Y from W&J Instrument CO., LTD. Mudu Jiangsu, China) with a continue RS-232 bus output configurated to never turn off (power save disabled) with the plastic foil between the bucket and the scale plate. A basic scheme depicts chamber and experimental setup function (Fig. 01). With this setup, the bucket mass diminution (enclosed soil water evaporation) was relatively well monitored and provided the real evaporation (*ER*) in the isothermal conditions.

An external fan blows the air on the chamber and an ultrasonic anemometer WindSonic 2D (Gill Instruments Limited, Lymington Hampshire, UK) allows monitoring and recording on the data logger CR1000 the resulting wind speed 5cm above the sample soil surface. It should be noted that $2ms^{-1}$ measured 5cm above the surface equals to about $6.5ms^{-1}$ measured 2m above the surface (logarithmic profile).

The data logger CR1000 was programmed to command closure (chamber head deployment) or opening of the chamber, to record the measured humidity and temperature along with the pressure, and the embedded fan rotation speed inside the chamber head as well as the wind speed before and during the deployment. Before each chamber deployment, a prior 120s flushing with a 100% duty operated embedded fan was performed. Between each PWM change for measurements, the chamber was opened, flushed during one minute and then closed again. Every six hours, a measurement cycle was initiated. Any measurement cycle consists to measure the absolute humidity accumulation in a closed chamber head with the embedded fan powered from PWM=10% duty to PWM=100% duty by step of 10% giving then ten consecutives chamber deployments. Each chamber deployment for each PWM takes about 10 minutes. With a flushing time between the deployments, the whole cycle takes over two hours. The six hour delay between each measurement cycle was adopted in order to do not strongly perturb the natural evaporation process. This protocol and ten different PWM measurements are for the fan influence characterization study purpose only. The real measurement protocol, as described below, is much shorter allowing more frequent chamber deployment.

The studied soil is either sandy, means a rough sand (0.1-3mm) or clayey (high clay content soil 50% clay, 40% silt, 10% sand). Real evaporation is deduced by weighting bucked with the studied soil calculating its mass M_B variation provided by the scale. The mean soil moisture w was determined by the ratio

$$w = \frac{(M_B - M_0)}{M_s}$$

(1)

With M_0 being the bucket with dry soil mas and M_s being the dry soil mass (without the bucket mass). This definition, gravimetric water content, is not a usual volumetric water content but often used for clayey soils since the soil volume changes and the cracking formation yields to a very complicated volume calculation.

Indeed, an additional difficulty concerns the volume determination for clayey soils as the volume is subject to change with the soil moisture content (swelling soils). Additionally, the crack apparition makes the volume determination and even its definition particularly difficult. Are the crack part of the soil sample or not? For these studies, the gravimetric water content is more usable.

2.3 Accumulation calculations

In order To estimate the water vapor efflux by the *NSS* technique, the absolute water vapor concentration q is monitored. Measured concentration versus time gives a curve regressed by an Exponential Rise (*ER*) formula very widely presents in all physical process as it is reflecting a variation versus time dC/dt, C being the scalar of interest, proportionally to the gap between the instant scalar value and the stable limit value C_l, that the scalar tent to reach:

$$\frac{dC}{dt} = k(C_l - C)$$

(2)

This differential equation has a general solution of the form:

$$C(t) = Ae^{-kt} + B$$

(3)

with A and B being constants.

With initial and final conditions, we can determine these constants using C_0 the initial value and τ the characteristic time also called response time ($\tau = \frac{1}{k}$) :

$$C(t) = C_l - (C_l - C_0)e^{-t/\tau}$$

(4)

The Evaporation Rate or Measured Evaporation *ME*, by definition, is determined by temporal derivation of the water vapor concentration q:

$$ME = \left(\frac{dq}{dt}\right)_{t=0}$$ (5)

It is important to note that the water vapor (and others gas emanating from the soil) accumulation inside the deployed chamber head is not constant. Only the initial evaporation rate (t=0 it means at the chamber head deployment beginning) is retained. In brief, the scale is allowing the Real Evaporation (*RE*) measurement and sensor monitoring closed chamber head space air moisture is allowing the Measured Evaporation (*ME*) determination by *ER* fit and time derivative. The calibration process is to compare *ME* with *RE*.

2.4 Automatized calculations algorithms

Used regression functions enforce the Levenberg-Marquardt algorithm for the *ER* fits on the whole acquired interval and singular value decomposition (SVD) algorithm giving residuals for polynomial fits with the least square method for optimizing fitting parameters. Then, the calculated polynomial roots are determined by a function based on a Riders algorithm. The first root gives the starting point (first cross point between the real measurement curve and the *ER* regressed curve) and the third root (third cross point) gives the limiting time for new *ER* fit.

3 Result and discussion

Soil evaporation measurement technique described in this paper is based on an adapted NSS technique principle. Used sensors characteristics, exact chamber configuration, regression calculations and wind influence are of a great importance.

3.1 Adaptation of dynamic closed NSS chamber

This technique is known since almost one century, described firstly first by Bornemann in 1920 and used for measurements of a trace gas efflux such as CO_2, N_2O or CH_4. Its operation operating principle is simple and consists to monitor of monitoring the rise in the gas of interest concentration rise when a well delimited soil part (delimited by an inserted collar) is covered by a cloche (chamber head). Numerous variants of this technique are used and for trace gas efflux measurements, continually improved and described such as: respiration chambers: Pavelka et al :(2018),Open Top Chambers: Fang and Moncrieff (1998) or Forced-Diffusion Chambers: Risk et al. (2011).

- Respiration Chambers: Pavelka et al. (2018),
- Open Top Chambers: Fang and Moncrieff (1998)

- Forced Diffusion Chambers: Risk et al. (2011).

The NSS technique is invasive, and the conditions of the measurements may be different from the real conditions, meaning "not chamber head deployed" conditions. This difference may affect the measurements. Then, for precise measurements, we must minimize the differences if we can or correct the measurements.

General issues concerning ~~the~~ closed chamber ~~technique~~techniques, construction, ~~operations~~operation and wind speed corrections ~~are~~will be listed elsewhere. In this paper, only special issues and solutions concerning ~~notably~~ the evaporation chamber ASERC technique corrected versus the wind speed are reported explicitly, but the experimental setup also ~~includes~~ implicitly includes some general solutions adopted for the closed chamber technique.

~~NSS chambers technique needs to be carefully considered for the water evaporation measurement use, but when correctly used, it can provide valuable data. The~~

A usual assumption ~~concerning this technique~~ concerns ~~the~~ soil efflux, which results from the migration of the gas of interest ~~migration~~ through the soil ~~supposed~~, assumed to ~~follow a~~be pure molecular diffusion ~~regime~~as described by ~~the~~ Fick's laws. However, ~~the evaporation efflux is a mass flow as during the evaporation, it means during the~~as liquid water is transformed into gaseous water ~~to water~~ vapor ~~transformation~~during evaporation, the volume is strongly increased ~~(about~~by approximately 1250-fold~~) which is moreover all vapor machines operation base. Then~~. Evaporation efflux is then a mass flow, not a diffusion, A device allowing an additional gas volume to ~~escape~~emerge from the soil ~~to~~into the chamber head ~~but do~~ not ~~rising~~raising the internal pressure as well, needs to be implemented ~~on the chamber.~~. Different solutions are possible and actually concern all the closed chambers since ~~the~~ soil evaporation ~~process~~ is always present even if ~~the~~ water vapor is not the gas of interest. One of the most commonly used devices is ~~a~~an open vent tube, which gives rise to another problem: the Venturi effect ~~(Xu et al 2005, Bain et al. 2005, Suleau et al. 2009).~~, listed later in this text as wind speed-induced influence. Another solution consists of an expansion room implementation ~~which~~that allows ~~to expand~~expansion of the chamber head volume while maintaining the internal pressure in equilibrium with the external air pressure. The expansion room is not subject to the Venturi effect. The late solution was then adopted for ASERC.

~~3.1.1 Sensors~~

~~The evaporation process is relatively fast and then, the humidity sensors should be even faster otherwise the deduced efflux may be biased. Fig. 02 (a) shows the accumulated effluxes measured by three sensors with a different response time. As we can see, a different response time of different sensors biases results thereof. A simple simulation, Fig. 02 (b), of a signal given by a sensor with more or less slow response time along with an artificial start delay imposed by the operator (in the case of a leading pipes, we have to wait after the chamber deployment before to record air analysing data from a distant analyser) and shows a possible underestimation but also overestimation of deduced efflux. Such overestimation may be committed with a relatively fast (as P14 Rapid) but not very fast sensor (as FTUTA 34) and a long recording time. As the signal deformation arises mainly at the beginning, during the recorded data regression, the first points importance will be overcome and the best~~

~~fit will be accorded to the further points increasing artificially *ER* amplitude and then the deduced flux. This possible overestimation vanishes with delay which results from the leading pipes or from a not instantaneous head space air mixing as shown later in this text. In the case of the leading pipe presence, the imposed time delay depends on the pipe's diameter and the air flow value. Flowing air is always mixed with pipe's enclosed air making calculated time delay rather approximative and not very well defined. An embedded sensor is always preferable. The fastest reliable air moisture and air temperature sensor used is a P14 Rapid (response time τ_{63} < 1.5s) on a Linpicco plate holding a PT1000 sensor providing simultaneous humidity RH (%) and air temperature Ta (°C) measurement.~~

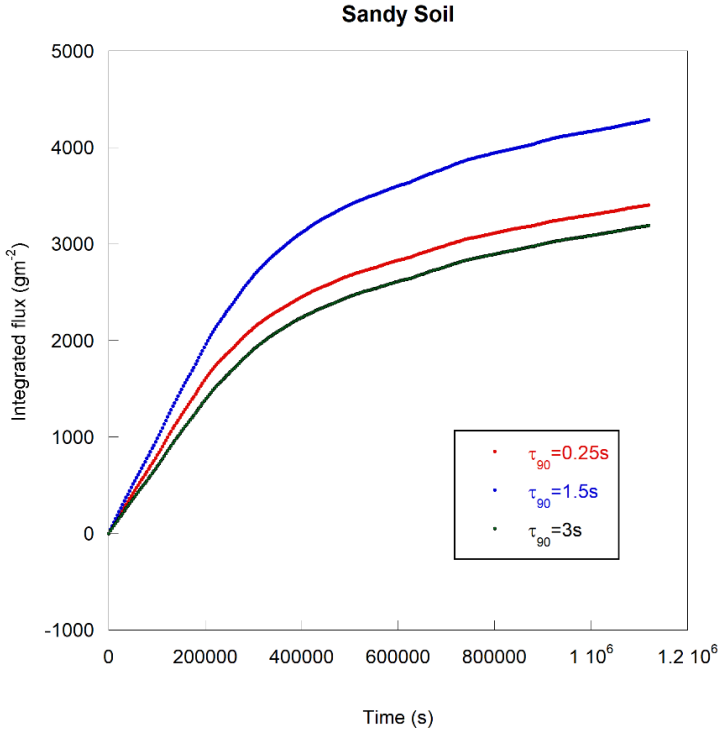

~~(a)~~

(b)

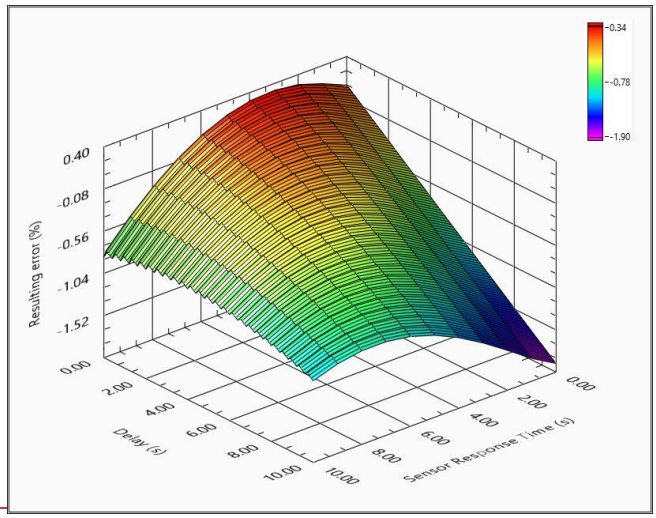

Figure 02: (a) **Integrate *ME* given by tree different sensor with different response time. BME280 and 3s response time, P14 Rapid with 1.5s response time and F-Tuta 34 which has the faster response time of 0.25s, unfortunately this sensor present quickly malfunctions and then was discarded. (b) Simulation of the *ER* regression error due to a slow sensor and introduced waiting delay with origin of time change.**

A simple calculation based on an empirical water saturation pressure versus temperature law published by Wagner (1995) gives the absolute humidity q (g/m^3). This formula is accurate to within 0.1% over the temperature range −30°C to +35°C:

$$q = \frac{13.2471488 \times e^{\frac{17.67 \times Ta}{243.5 + Ta}} \times RH}{273.15 + Ta}$$

device allows equalization of the internal (6)

An external sensor such as Infra-Red Gas Analyzer (IRGA) provides better accuracy but requires a leading pipe use between the chamber head pressure and external ambient pressure even if the IRGA with an external pump. The leading pipes may seriously bias the measures by adsorption problems, condensation problems and time lag between the chamber closure and the corresponding air sample measure, additionally to the heating problem since the IRGA is heating the analysed air sample which is reinjected back to the chamber head and needs then to be cool downpressure is changing, which is important to preserve the external turbulence influences.

All internal metallic parts were coated with a high polytetrafluoroethylene (PTFE, i.e., Teflon) content paint to reduce the water vapor sorption on a metallic surface as much as possible and to not affect the initial *RH*.

Inside the collar was inserted a pipe allowing the air entrapped by the chamber head during chamber deployment to flow freely through to a nitrile finger cot (expansion room) to equilibrate the inside and outside pressure and allow a small chamber volume expansion to compensate for the mass flow from the soil. Compared to the chamber head volume, during chamber head

deployment, the volume increase is very small and does not bias the calculations. This expansion room also allows equal pressures inside and outside the deployed chamber head, which is important for pressure pumping conservation (described later in the text).

As heating from solar radiation may strongly affect the evaporation process by artificially raising the chamber head temperature, special attention is given to shielding the chamber head with a first albedo shield made from a white painted stainless-steel plate. This shield screens direct radiation; however, its temperature will rise, and its infrared radiation may reach the chamber head as well. A well-known technique used for cryogenic fluid operation was then adapted by interposing a second infrared (IR) shield made from a plastic plate coated with a thick aluminum foil on both sides. In this way, the closed chamber head internal temperature is assumed to be equal to the external ambient temperature.

2.2 Measurement protocol

For all the calibration measurements, the chamber was placed on holds, and the collar bottom, normally inserted into the soil, was hatched with elastic plastic foil. An electronic scale was placed just below this foil, and a bucket with a studied soil was placed inside the collar reposing on the scale configured to never turn off (power save disabled) with the plastic foil between the bucket and the scale plate. A basic scheme depicts the chamber and experimental setup function (Fig. 01). With this setup, the bucket mass diminution (due to enclosed soil water evaporation) was relatively well monitored and provided real evaporation (*ER*) under isothermal conditions.

An external fan blows the air on the chamber, and an ultrasonic anemometer WindSonic 2D (Gill Instruments Limited, Lymington Hampshire, UK) allows monitoring and recording (on the data logger CR1000) the resulting wind speed 5 cm above the sample soil surface. The 2 ms^{-1} measured 5 cm above the surface equals approximately 6.5 ms^{-1} measured 2 m above the surface (logarithmic profile).

The data logger CR1000 was programmed to command closure (chamber head deployment) or opening of the chamber, to record the measured humidity and temperature along with the pressure, to control the embedded fan rotation speed inside the chamber head and to monitor the external wind speed before and during the deployment. Before each chamber deployment, a prior 120 s flushing with a 100% duty operated embedded fan was performed. Between each PWM change for measurements, the chamber was opened, flushed for one minute and then closed again. Every six hours, a measurement cycle was initiated. Any measurement cycle consists of measuring the absolute humidity accumulation in a closed chamber head with the embedded fan powered from PWM=10% duty to PWM=100% duty by steps of 10%, giving then 10 consecutive chamber deployments. Each chamber deployment for each PWM takes approximately 10 min. With a flushing time between the deployments, the whole cycle takes over two hours. The six-hour delay between each measurement cycle was adopted to avoid strongly perturbing the natural evaporation process. This protocol and ten different PWM measurements are for the internal

fan influence characterization study purpose only. The real measurement protocol, as described below, is much shorter, allowing more frequent chamber deployment.

The studied soil is either sandy, meaning rough sand (0.1-3 mm) or clayey (high clay content soil 50% clay, 40% silt, 10% sand). Real evaporation is deduced by weighing the bucket with the studied soil and calculating the corresponding M_B mass variation. Soil moisture w was determined by the ratio:

$$w = \frac{(M_B - M_0)}{M_s} \quad (1)$$

where M_0 is the bucket mass with dry soil, and M_s is the dry soil mass only (without the bucket mass). This definition, gravimetric water content, is not a usual volumetric water content provided by all soil water content (SWC) probes but is often used for clayey soils since the soil volume changes and the crack formation yields a very complicated volume calculation.

Indeed, an additional difficulty concerns the volume determination for clayey soils, as the volume is subject to change with the soil moisture content (swelling soils). Additionally, the crack appearance makes volume determination and even its definition particularly difficult. Are the cracks part of the soil sample or not? For these studies, the gravimetric water content is more usable.

~~The usual polyurethane (PU) pneumatics tubes were checked.~~ 2.2 Flux~~Fig. 03 (a) shows an apparent characteristic time variation of a measured absolute humidity rise by a fast IRGA (Li-840A, LI-COR Biosciences, Lincoln, Nebraska USA) on one edge of the leading pipes when a step like humidity rise or fall is induced (by a Li-610 portable dew point generator, LI-COR Biosciences, Lincoln, Nebraska USA) plugging or unplugging on the other edge of the leading pipes versus the length of the pipes. As we can see, the apparent characteristic time is increasing strongly with the leading pipes length reflecting a strong sorption problem with the PU pipes. Polytetrafluoroethylene (PTFE also called Teflon) pipes are preferable but need to be insulated anyway in order to prevent condensation possibility and induce always a lag problem between the chamber closure time and the incoming air sample time from the chamber to the analyser which needs to be precisely known as it may bias again the regression results.~~

~~An embedded fast and accurate sensor is then preferable.~~

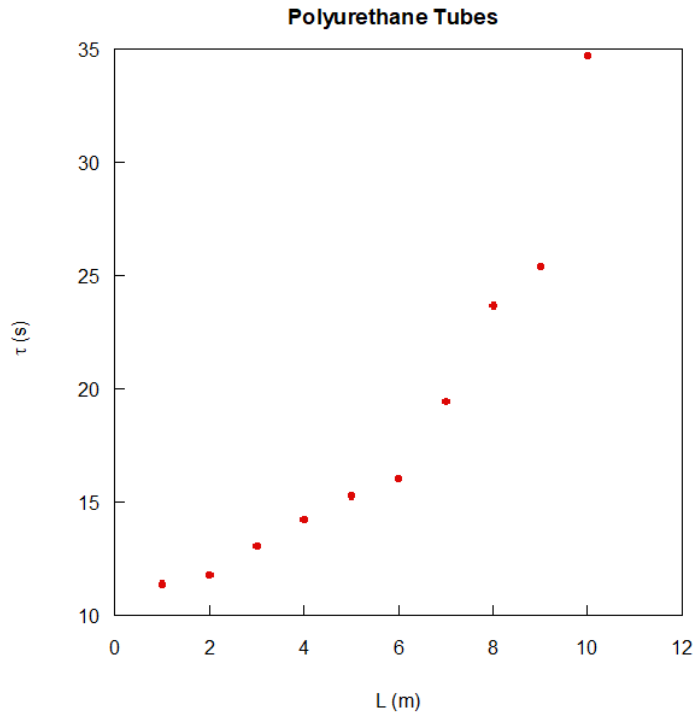

(a)

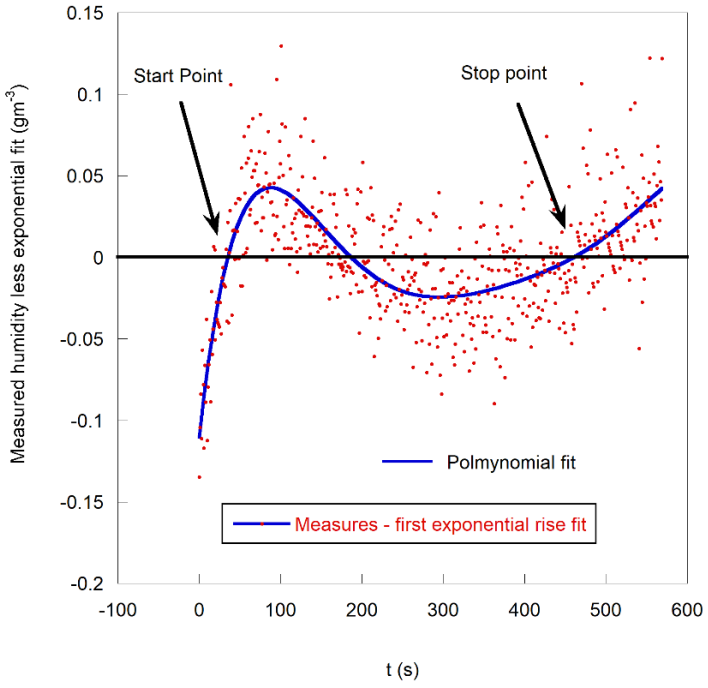

(b)

~~Figure 03: (a) Apparent response time of the polyurethane tubes versus the length of the tubes. (b) Measured absolute humidity less exponential fit (residuals) giving start and stop points for a second regression.~~

~~3.1.2 Regressions~~ calculation ~~methodology~~algorithms

To estimate the water vapor efflux by the *NSS* technique, the absolute water vapor concentration q is monitored. Measured concentration versus time gives a curve regressed by an exponential rise (*ER*) formula very widely presented in all physical processes, as it reflects a variation versus time dC/dt, where C is the scalar of interest and is proportional to the gap between the instant scalar value and the stable limit value C_l:

$$\frac{dC}{dt} = k(C_l - C) \quad (2)$$

This differential equation describes widely spread physical behavior and has a general solution of the following form:

$$C(t) = Ae^{-kt} + B \quad (3)$$

with A and B being constants.

With initial and final conditions, we can determine these constants using C_0 as the initial value and τ asthe characteristic time, also called response time ($\tau = \frac{1}{k}$) :

$$C(t) = C_l - (C_l - C_0)e^{-t/\tau} \quad (4)$$

This variation behavior is very often observed in nature, including electronic and sensor responses to measured variable C changes. Concerning evaporation rate or (*ME*), by definition, is determined by temporal derivation of the absolute water vapor concentration q multiplied by chamber head volume V and divided by chamber basis surface S:

$$ME = \frac{V}{S}\left(\frac{dq}{dt}\right)_{t=0} = \frac{V}{S}(q_l - q_0)/\tau \quad (5)$$

The water vapor (and other gases emanating from the soil) accumulation rate inside the deployed chamber head is not constant. Only the initial evaporation rate (t=0, which means at the beginning of chamber head deployment) is then retained (q_l is the absolute water concentration limit; q_0, is the initial absolute water concentration, and τ is the characteristic time of q evolution).

As in the case of all other soil trace ~~gases~~gas measurements, the measured absolute water vapor concentration rise in a closed chamber head is not linear with time but rather follows an exponential rise (ER) law. ~~As~~ Usually, due to the complexity of the

accumulation and feedback process, the exponential law does not ~~describe~~ perfectly describe the measurements, and some deviations are observed, making the regression results sensitive to the starting point, duration and ~~the~~ end point. This ~~is a general~~ observation is general, intrinsically tied ~~with~~to the closed chamber technique (Nakano et al~~.~~., 2004). Concerning water evaporation, ~~we can notice that~~ the measurement curve and the ER fit for a sufficiently long ~~enough~~ time present three well-defined cross points~~.~~ due to a noninstantaneous sensor measurement, as shown in Appendix B. For this study, ~~in order~~ to stabilize the numerical regression conditions (fit), the starting point is systematically chosen at the first cross point and the end point at the third cross point (Fig. ~~03~~02 (b)). In other words, a double fit is needed. A first fit on the whole disponible length provides the starting and the end ~~point~~points, and then, a second exponential rise fit is performed between these two points to provide every ~~seeking values.~~sought value. Only the result of the second fit is considered ~~as~~ reliable. Of course, in some cases, such as a very slow evaporation, we do not observe the third cross point. In these cases, the retained interval is between the first cross point and the last available point.

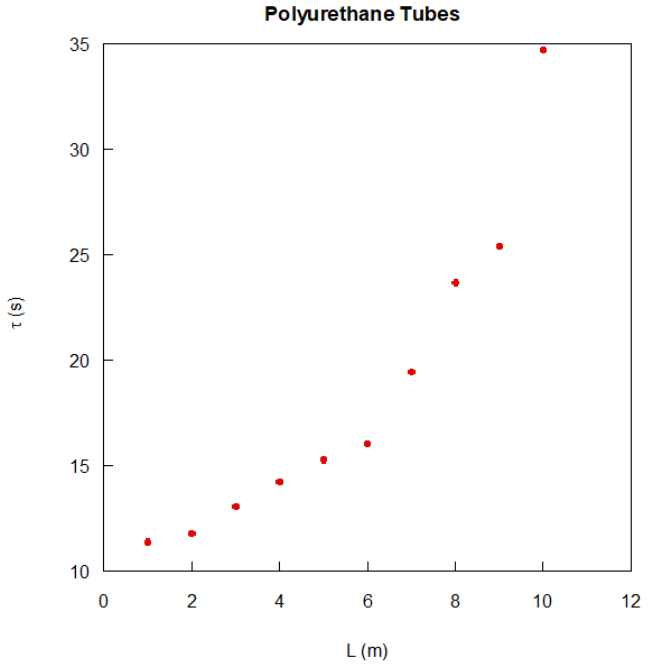

(a)

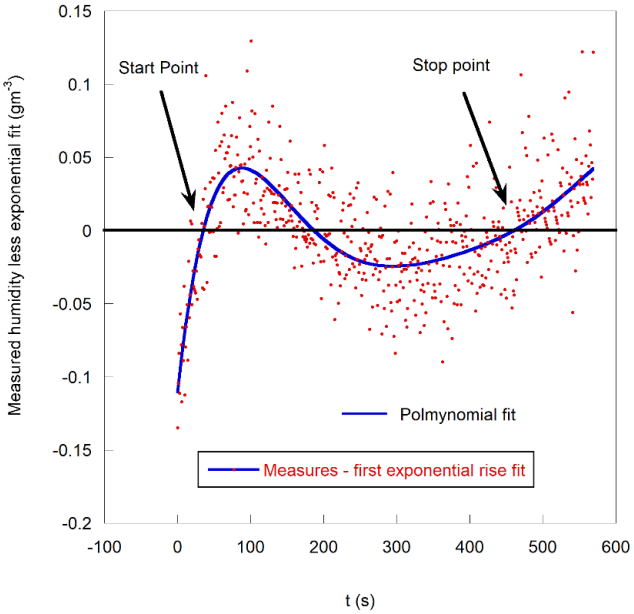

(b)

Figure 02: (a) Apparent response time of the polyurethane tubes versus the length of the tubes. (b) Measured absolute humidity less exponential fit (residuals), giving start and stop points for a second regression.

All calculations were automated using LabView 2015 programming (National Instruments Corporation, Austin, TX, USA). The regression functions enforce the Levenberg–Marquardt algorithm for the *ER* fits over the whole acquired interval, and the singular-value decomposition (SVD) algorithm gives residuals for polynomial fits with the least square method for optimizing fitting parameters. Then, the calculated polynomial roots are determined by a function based on a Riders algorithm. The first root gives the starting point (first cross point between the real measurement curve and the *ER* regressed curve), and the third root (third cross point) gives the limiting time for new *ER* fit.

2.3 Sensor characteristics

The evaporation process is relatively fast, and then, the humidity sensors should be even faster; otherwise, the deduced efflux may be biased. Fig. 03 (a) shows the accumulated effluxes measured by three sensors with different response times. Different response times of different sensors bias the results thereof. A simple simulation, described in Appendix B and depicted in Fig. 03 (b), calculates the signal given by a sensor with different response times along with an artificial start delay imposed by the operator (in the case of a leading pipe, we must wait after the chamber deployment before recording air analysis data from a

distant analyzer). As shown, a possible underestimation but also an overestimation of deduced efflux is observed. Such overestimation may be committed with a relatively fast (as in P14 Rapid) but not very fast sensor (as in FTUTA 34) and a long recording time. This possible overestimation vanishes with delay resulting from the leading pipes or from a slow head space air mixing delay, as shown later in this text. In the case of the leading pipe presence, the imposed time delay depends on the pipe diameter and the air debit importance. Flowing air is always mixed with the enclosed air of the pipe, making the calculated time delay rather approximate and not very well defined. An embedded sensor is always preferable. The fastest reliable air moisture and air temperature sensor used is a P14 Rapid (response time τ_{63} < 1.5 s) on a Linpicco plate holding a PT1000 sensor providing simultaneous RH (%) and air temperature Ta (°C) measurements.

A simple calculation based on an empirical water saturation pressure versus temperature law published by Wagner (1995) gives the absolute humidity q (g·m^{-3}). This formula is accurate to within 0.1% over the temperature range –30 °C to +35 °C:

$$q = \frac{13.2471488 \times e^{\frac{17.67 \times Ta}{243.5 + Ta}} \times RH}{273.15 + Ta} \quad (6)$$

An external sensor such as IRGA provides better accuracy but requires a leading pipe use between the chamber head and the IRGA with an external pump. The leading pipes may seriously bias the measures by adsorption problems, condensation problems and time lag between the chamber closure and the corresponding air sample measurement. Additionally, a heating problem arises since any IRGA is heating, thus necessitating cooling down the analyzed air sample reinjected back to the chamber.

The usual polyurethane (PU) pneumatic tubes were checked. Fig. 02 (a) shows an apparent characteristic time variation of a measured absolute humidity rise by a fast IRGA (Li-840A, LI-COR Biosciences, Lincoln, NE, USA) on one edge of the leading pipes when a step such as humidity rise or fall is induced (by a Li-610 portable dew point generator, LI-COR Biosciences) plugging or unplugging on the other edge of the leading pipes versus the length of the pipes. The apparent characteristic time increases strongly with the leading pipe length, reflecting a strong sorption problem with the PU pipes. Teflon pipes are preferable but need to be insulated anyway to prevent the possibility of condensation and always inducing a lag problem between the chamber closure time and the incoming air sample time from the chamber to the analyzer, which needs to be precisely known, as it may again bias the regression results.

An embedded, fast and accurate sensor is then preferable.

Once the experimental setup was truly built, the operation condition was chosen ~~and~~, the regression points stabilized, and the wind speed influence was studied. The scale allows the real evaporation (*RE*) measurement and sensor monitoring of closed chamber head air moisture, allowing the measured evaporation (*ME*) determination by *ER* fit and initial slope calculation. Calibration lies in the comparison between *ME* and *RE*.

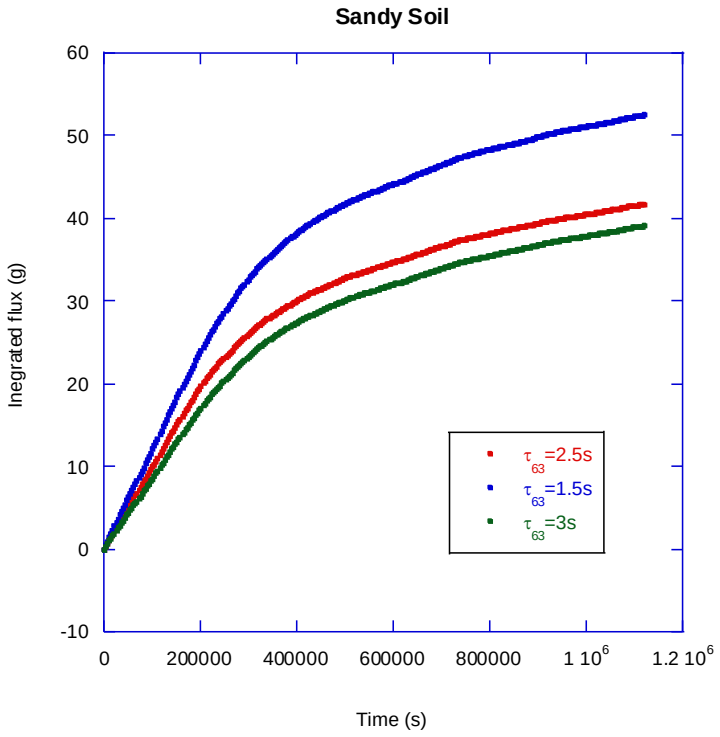

(a)

~~3.1.3 Wind influence considerations~~

~~The wind influence on the water vapor efflux is well known and widely studied (Thornthwaite and Holzman 1942, Hanks and Woodruff 1958). Even if a non diffusive regime for a soil evaporation process was explored more than a half century ago (Fukuda 1955), studies which considered a gustiness wind influence from the theoretical point of view by a sinusoidal representation and concluded to a negligibility of the phenomenon, others authors studied and experimented the wind influenced evaporation (Farrell et al. 1966, Scotter and Raats 1968) and concluded, on the contrary, to a great importance of a non-diffusive regime. Recently, numerous authors, experimentally and theoretically studding the gas propagation in the porous media, have pointed out an important or even biggest role of the non diffusive regimes such as thermal and solutal dispersion (Davarzani et al. 2014), convection and advection or pressure fluctuations for gas movement through porous media (soil) see Sánchez-Cañete et al. (2016) and the references given by them. One of a major gas movement cause is the so-called wind pumping which includes three effects:~~

- ~~Venturi effect (Xu et al. 2005, Bain et al. 2005, Suleau et al. 2009) giving rise to a mass transfer by pressure gradient establishment.~~

- Natural gradient concentrations disturbance (Le Dantec et al. 1999, Longdoz et al. 2000, Lai et al. 2012) playing an important role during very calm conditions and a highly stratified boundary layer slowing down the diffusion efflux and, once disturbed, by the head space fan mixing releasing an unusual high apparent efflux.
- Eddy pressure fluctuations causing gas dispersion (Maier et al.2010, Mohr et al. 2016, Brændholt et al. 2017, Pourbakhtiar et al. 2017, Poulsen et al. 2017, Mohr et al. 2017) that may be of a very important gas transport regime. This effect is more or less screened by the chamber deployment mainly depending on the wind importance versus the head space mixing fan disturbances.

All these effects are altered by a deployed chamber head and then affect the closed chamber measurements versus a natural soil efflux. As the wind cannot be reproduced inside the chamber heads, the only possibility is to correct the data calibrating the measurements versus the wind which is the aim of this paper presenting a non steady state dynamic chamber technique adapted and wind corrected for the water vapor efflux measurement.

3.1.4 Modeling difficulties

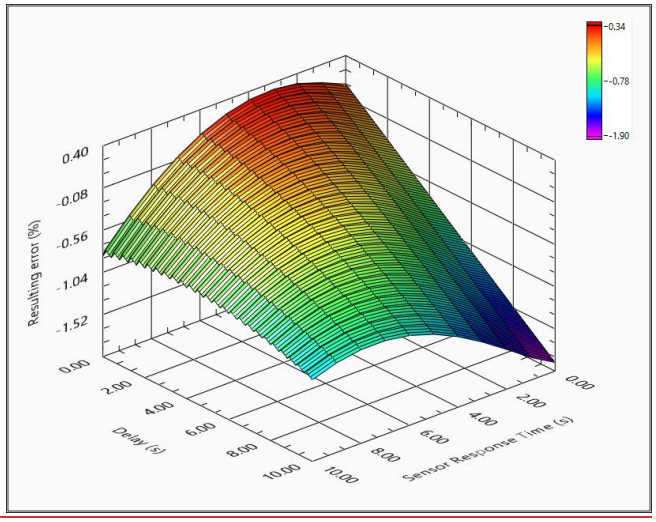

(b)

Figure 03: (a) Integrated *ME* given by three different sensors with different response times. BME280 and 3 s response time, P14 Rapid with 1.5 s response time and F-Tuta 34 which has the faster response time of 0.25 s. Unfortunately, this sensor quickly malfunctioned and then was discarded. (b) Simulation of the *ER* regression error due to a slow sensor and introduced waiting delay with the origin of the time change.

4 Results and discussion

The soil evaporation measurement technique described in this paper is based on an adapted NSS technique principle. The sensor characteristics, exact chamber configuration, regression calculations and wind speed influence are of great importance. As special attention was given to the design of the chamber to avoid affecting the internal chamber head temperature by solar radiation screening and IR radiation screening and to not affect the pressure variations incorporating an "expansion volume", the differences in the temperature or the pressure inside the chamber head or outside were quite similar. In other words, chamber measurements do not have to be corrected versus temperature or pressure. The initial air humidity is also assumed to be the same, as the chamber fan is engaged just before chamber head deployment to flush the sensor. Only air movements cannot be preserved, and their influence on soil evaporation must be corrected

The wind influence on

~~The wind influence on the~~ soil evaporation depends on numerous variables ~~such as~~, such as the soil temperature and moisture, the air temperature and the humidity, as well as the soil ~~temperature and moisture, the air temperature and the humidity but also the soil nature~~composition and the soil texture. These variables may change more or less quickly, and some of them, such as the soil texture, are not ~~real-time~~ monitorable~~.~~ in real time.

~~In others words~~Consequently, even if we succeed ~~to model~~in modeling the wind effect, we will not be able to use ~~it~~this wind effect for ~~chambers~~chamber data corrections. An ~~auto-calibrating~~autocalibrating chamber would be considered ~~as~~ a solution. The target is not to measure every variable and inject it into a complex model but rather to measure the "susceptibility" of the soil evaporation to the wind and correct the chamber measurements against the measured wind. The following protocol gives very ~~simples~~simple yet relatively accurate results.

~~3~~4.1.~~5~~ Fundamental finding

At a fixed internal fan speed (PWM constant), the measured water vapor efflux (*ME*) is not directly proportional to the real water vapor efflux (*RE*) during a soil drying process ~~at~~with a stable wind (Fig. 04).

This ~~non-linearity~~nonlinearity changes with the soil ~~nature~~composition and even with the soil texture ~~is~~, making it impossible to correct any data for all soil ~~natures~~compositions and textures with a unique formula based only on the wind speed.

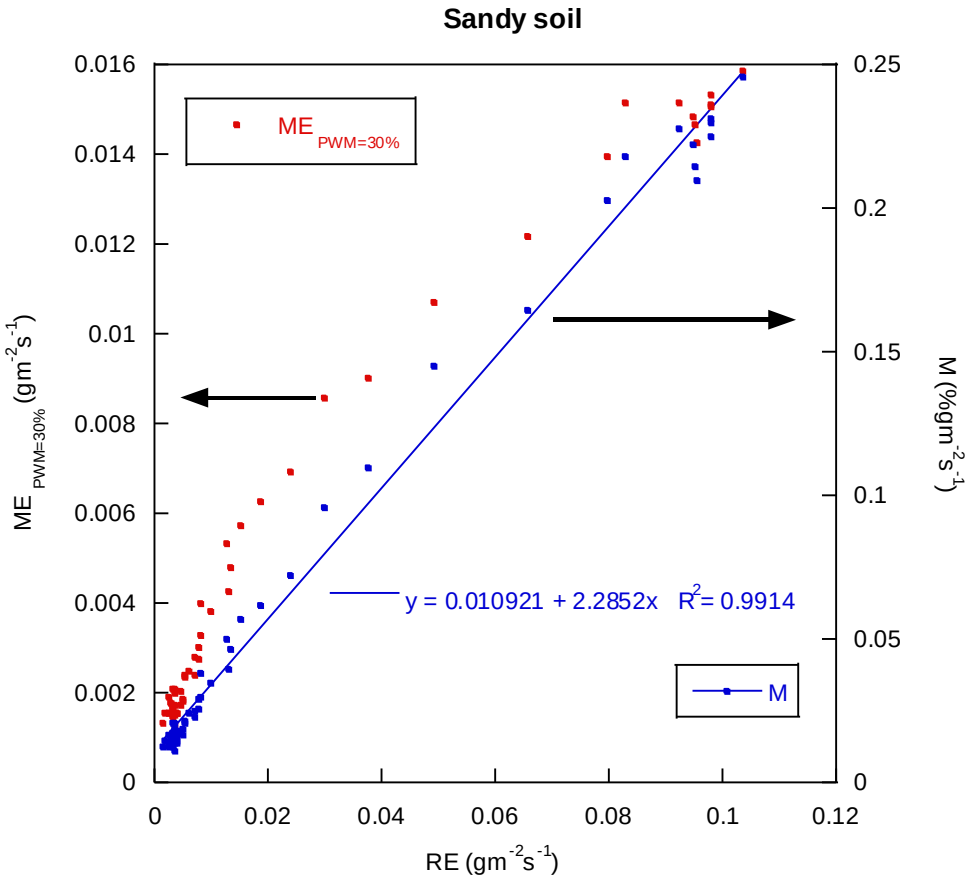
Sandy soil
ME PWM=30%
y = 0.010921 + 2.2852x R2= 0.9914
M
ME PWM=30% (gm-2s-1)
M (%gm-2s-1)
RE (gm-2s-1)
0.016
0.014
0.012
0.01
0.008
0.006
0.004
0.002
0
0.25
0.2
0.15
0.1
0.05
0
0.02
0.04
0.06
0.08
0.12

605

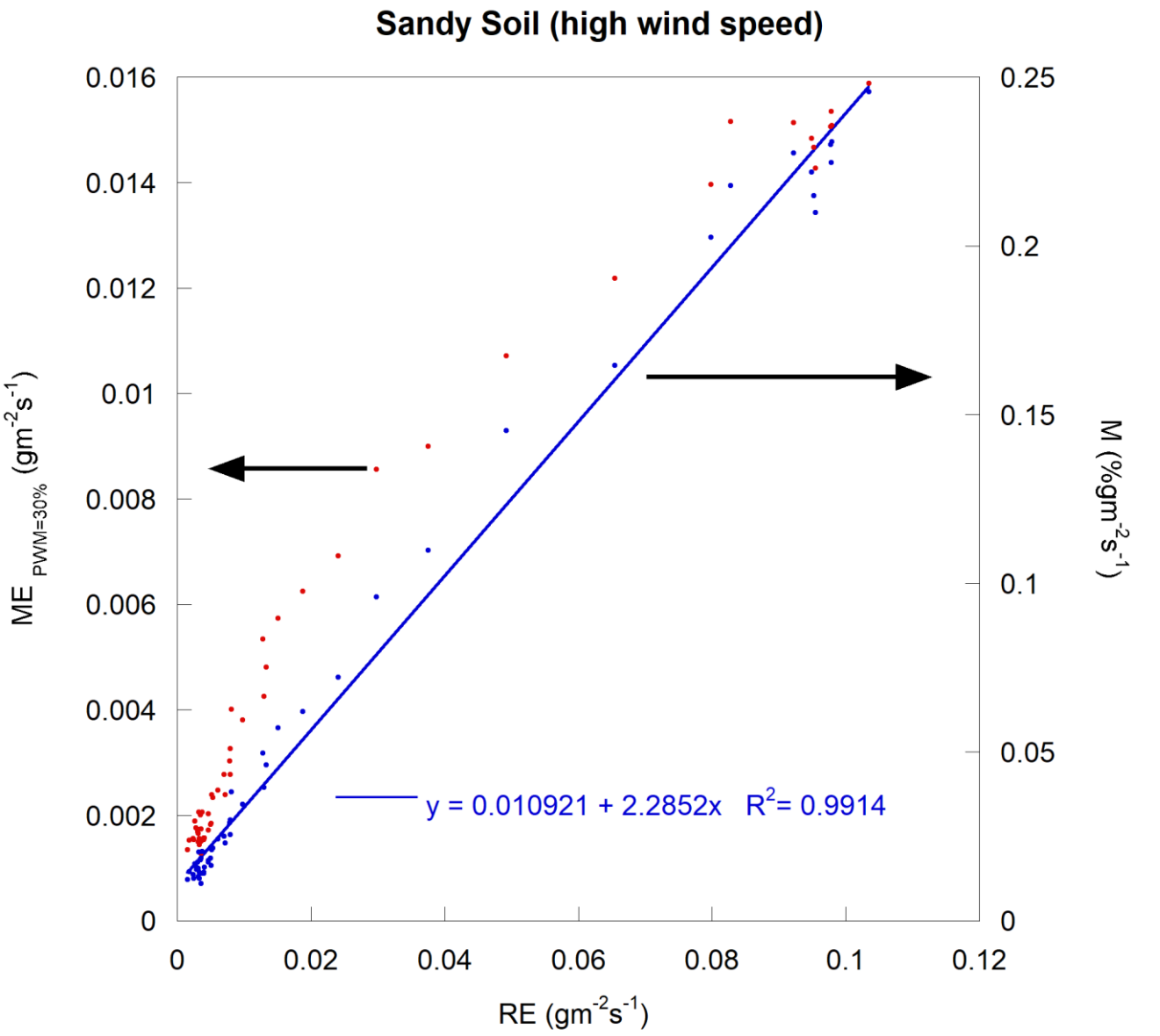

Figure 04: ~~Measure~~**Measured evaporation versus real evaporation (red dots on the left side axis) and M, averaged measure multiplied by the Z factor, along with a linear regression (blue dots on the right-side axis) for sandy soil under a 1.~~~~15ms~~**15 ms^{-1} wind speed.**

610

~~3.1.6~~4.2 Embedded fan influence check

~~As we can see,~~Figure 05 also shows the recorded water vapor efflux with sandy and clayey soil versus the fan PWM duty control. Both soil results are very well described by an exponential law:

$$ME(PWM) = A * e^{-Z/PWM} \quad (7)$$

A and Z are constant for a given soil sample and external conditions. In the adopted chamber head configuration, the internal fan influence is similar to the external wind influence. Similar~~,~~ but not identical since the wind brings some fresh air when a fan can only mix the internal head space air with a progressively rising water vapor concentration. ~~Figure 05 shows also the recorded water vapor efflux with a sandy and a clay soil versus the fan PWM duty control. As we can see, both soils results are very well described by an exponential law:~~

~~$$ME(PWM) = A * e^{-Z/PWM} \quad (7)$$~~

~~A and Z being constant for a given soil sample and external conditions.~~

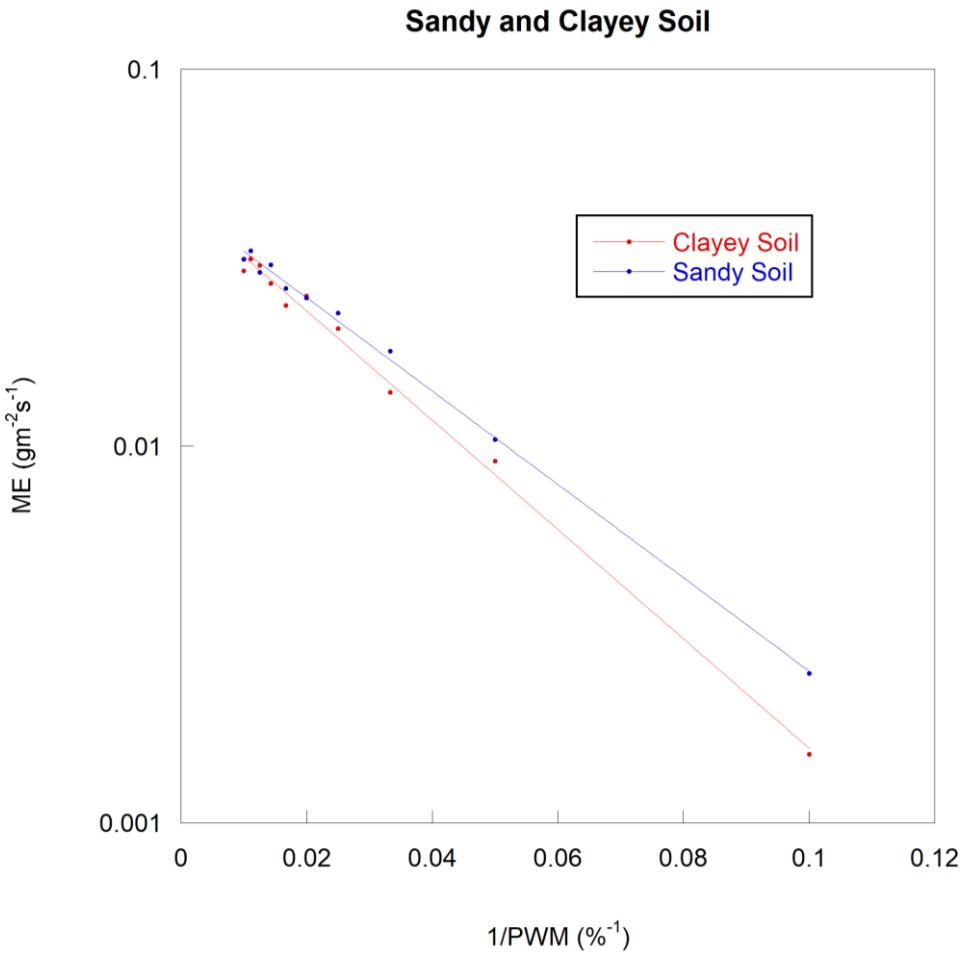
Sandy and Clayey Soil
0.1
0.01
0.001
ME (gm-2s-1)
0
0.02
0.04
0.06
0.08
0.1
0.12
1/PWM (%-1)
Clayey Soil
Sandy Soil

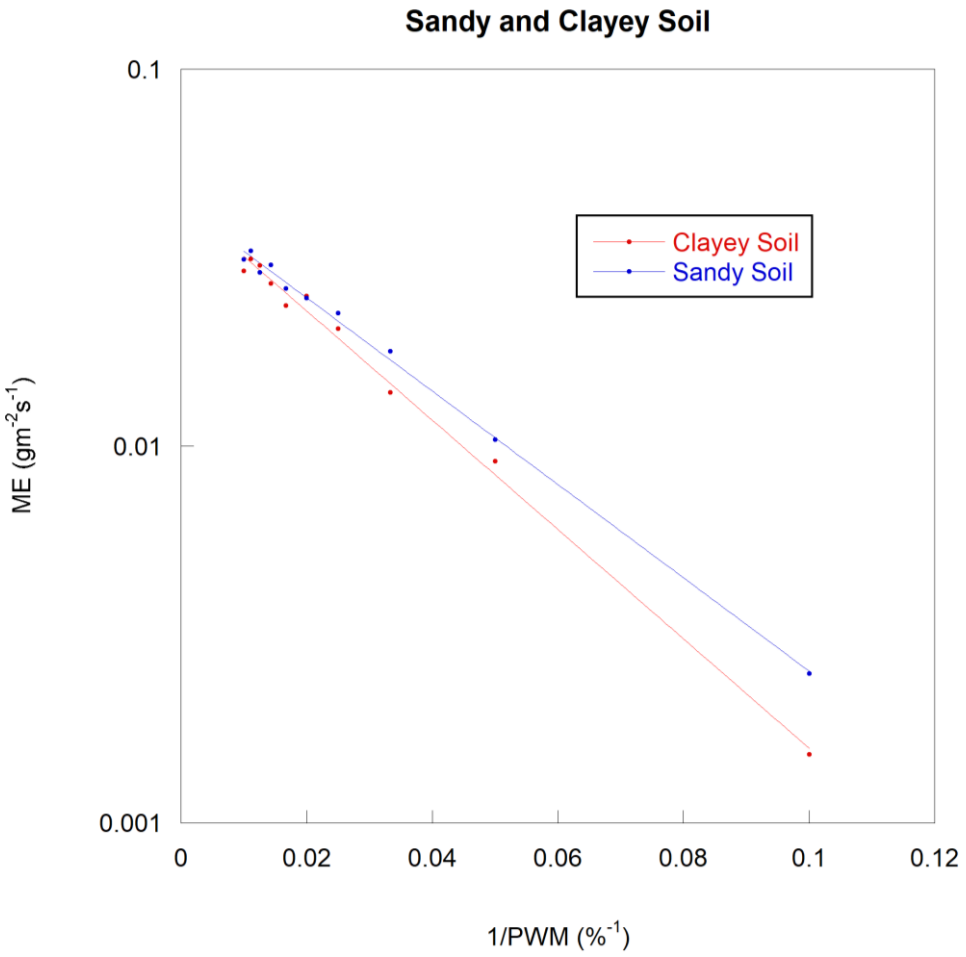

Figure 05: Measured evaporation versus 1/PWM for sandy soil under 0.~~72ms~~72 ms^{-1} wind and for clayey soil under 0.~~8ms~~8 ms^{-1} wind speed.

The constant *A* ~~is reflecting~~reflects the amplitude of the evaporation for a given soil and weather conditions, and the constant *Z* ~~is reflecting~~reflects a soil susceptibility to the internal fan mixing flow. By similitude, one can assume *Z* ~~reflecting~~reflects the soil evaporation ~~wind~~ susceptibility to the wind speed.

~~In order~~ To determine *Z*, the most effective way is to perform numerous measurements with a different *PWM* value and apply an exponential regression to all these results (Z_{total}). However, this ~~way~~method is long, and resulting perturbations do not allow a high sampling rate. Two-point measurements used for *Z* determination are of a relatively ~~of a~~ good concordance if the first fan speed used is low, such as *PWM* = 10~~%~~%, and the second speed is significantly higher, such as PWM = 30% (Fig. 06).

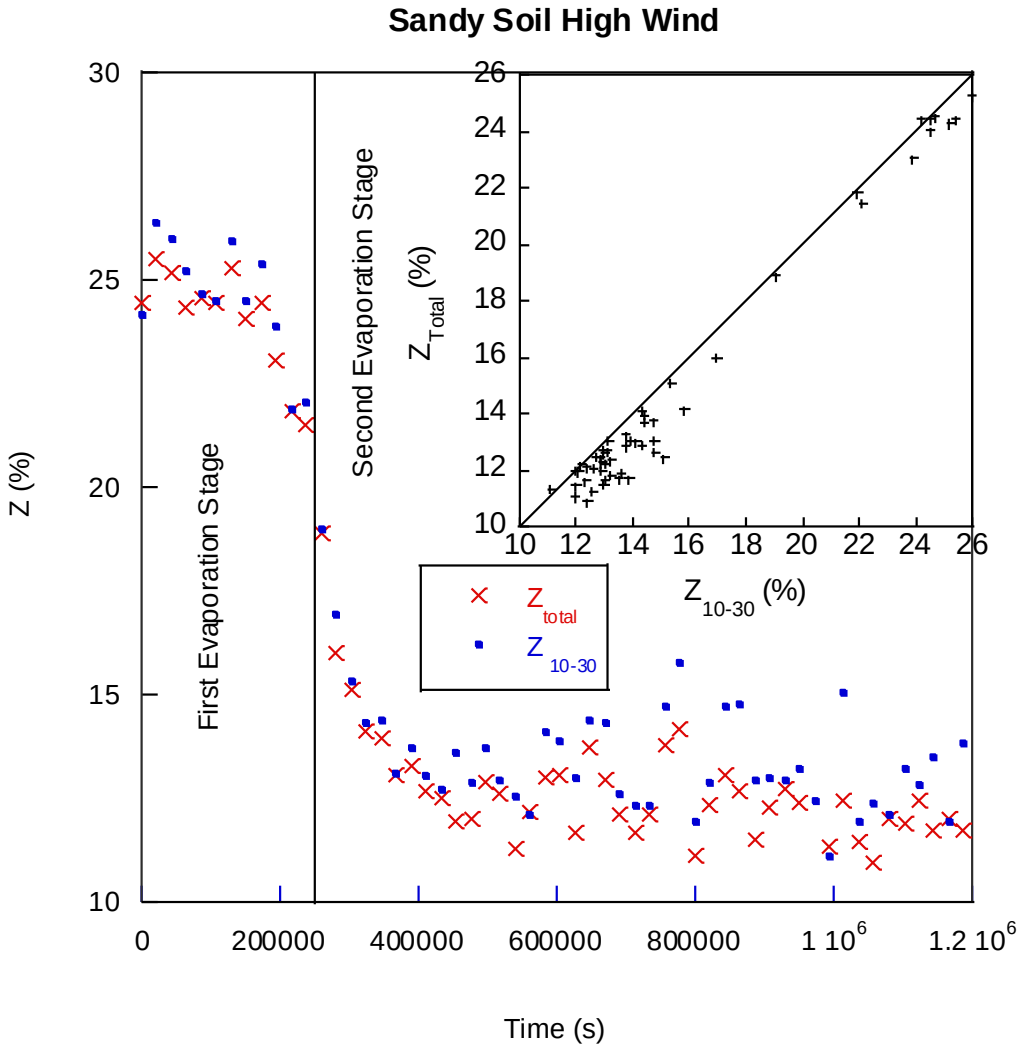
Sandy Soil High Wind
Z (%)
Time (s)
First Evaporation Stage
Second Evaporation Stage
Z_Total (%)
Z_10-30 (%)
Z_total
Z_10-30
30
25
20
15
10
0
200000
400000
600000
800000
1 10^6
1.2 10^6
26
24
22
20
18
16
14
12
10

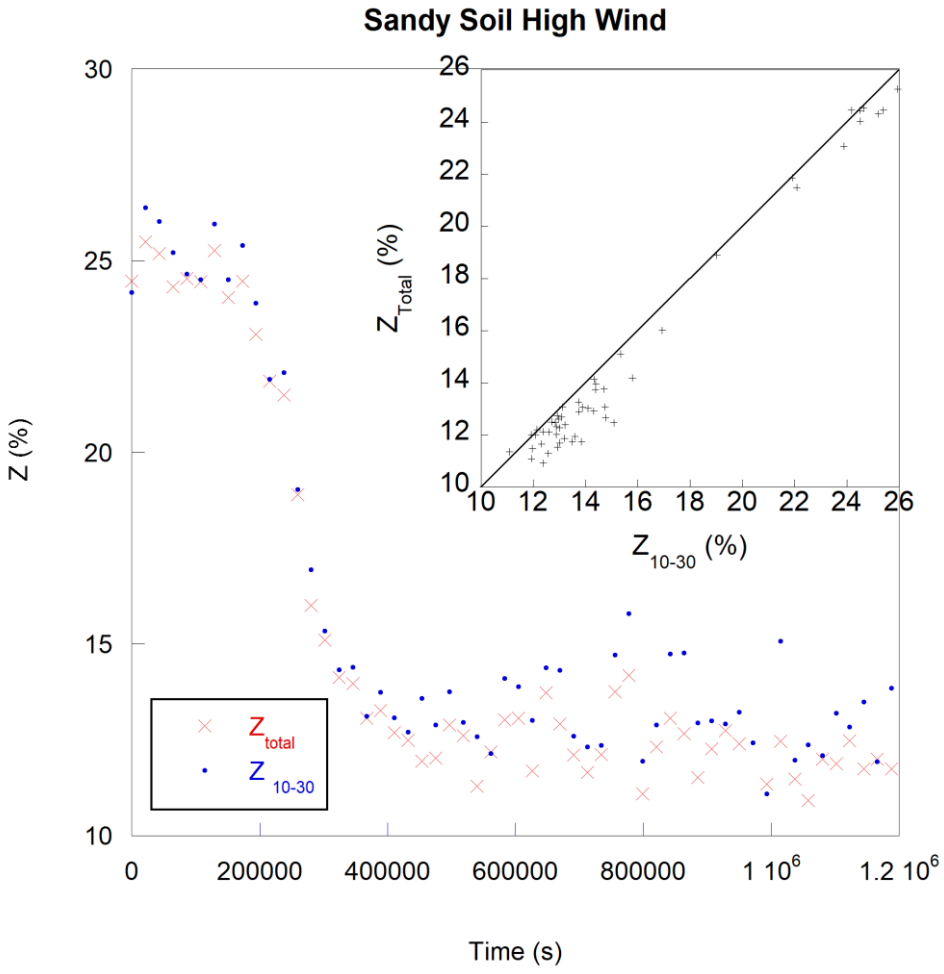

Figure 06: Z_{total} and Z_{10-30} versus time for sandy soil at a relatively strong wind of 1.~~15ms~~15 ms^{-1}. Insert, the same values of Z_{total} versus Z_{10-30}.

A visible *Z* drop between the first evaporation stage and the second evaporation stage is observed. The best results for a correction were given by the function *M*, which is the average of ME_{10} measurements at *PWM* = 10% and ME_{30} measurements at *PWM* = 30% multiplied by Z_{10-30} obtained by an exponential regression of the two-point measurement ME_{10} and ME_{30} versus 1/*PWM* by an exponential ~~function 6~~Eq. 7:

$$M = \frac{ME_{10} + ME_{30}}{2} * Z_{10-30} \quad (8)$$

~~As we can see on the Fig.~~ Figure 04~~, the~~ shows that *RE* is ~~near~~nearly proportional to *M* (defined by ~~formula 7~~Eq. 8) and~~, which is the main benefit of Z introduction,~~ Fig. 07 shows that this proportionality constant, called thereafter *m*, depends ~~mainly~~ on the wind speed ~~w_S~~ and ~~remains unchanged whatever is~~not on the soil ~~nature, texture, moisture or temperature as shows Fig. 07.~~composition, which is the main benefit of *Z* introduction. Only *M* depends on the soil ~~nature,~~ composition, soil texture or soil and air meteoritical variables ~~what is included in the~~pertinent for soil evaporation measurements.

$$RE = m(w_S) * M + B \quad (9)$$

B is a constant~~,~~ of a very small amplitude useful only for ~~a very small wind speed or a~~ very dry soil.

We can then decompose the Eq. 9 in three terms:

- $m(w_S)$ is a correction coefficient that depends only on the wind speed, the only pertinent variable affected by the chamber head deployment.
- $M_{10-30} = \frac{ME_{10}+ME_{30}}{2}$ reflects soil evaporation depending on all pertinent variables, such as SWC, air water vapor demand, air and soil temperature, and pressure, which are not affected by chamber head deployment under fixed boundary layer air movement.
- *Z* reflects the soil evaporation susceptibility to the wind speed, as with the same wind speed, soil evaporation is not the same depending on the soil composition, soil texture, etc.

The *m* dependence of the wind speed is not trivial. The plateau ~~around~~at approximately *w* = 0.~~5ms~~5 ms^{-1} probably corresponds ~~probably~~ to the fan ~~perturbations~~perturbation concordance at *PWM* = 20% (an average between PWM=10% and PWM=30%) comparable to the wind speed of 0.~~5ms~~5 ms^{-1} ~~speed~~ perturbations. This particular value is tied ~~with~~to the chamber design and cannot be used as a universal value. The other limitation is the high wind speed. As ~~shows~~shown by Smits ~~and~~et al. (2015), for ~~the~~ wind ~~speed~~speeds superior to a threshold value W_{Smax}, the evaporation process is not much more affected by ~~the~~ wind. Then, *m(~~w~~W_S)* is probably no ~~more~~longer linear with $W_S > W_{Smax}$.

For the studied range of the wind speed, the adopted adjustment formula for $m(W_S)$ is of the form:

$$m(\sout{w_S})(W_S) = \frac{\sout{a * w_S}}{\sout{e^{b/w_S}}} \frac{a * W_S}{e^{b/W_S}} + c(1 - \sout{e^{-d*w_S}} e^{-d*W_S}) + g \quad (10)$$

with a, b, c, d and g constants determined empirically.

As a validity check for the studied wind speed in the range of zero to ~~2ms~~2 ms^{-1}, Fig. ~~08~~08 a) shows all raw data (*RE* versus uncorrected $ME_{10\text{-}30}$ (average of ME_{10} measured with *PWM*=10%, and ME_{30} measured with *PWM*=30%) used for calibration,

and Fig. 8 b) shows all the available data corrected using $m(Ws)$; the unique function for the composition of all ~~soils' nature~~soils and texture depending only on the wind speed. ~~The~~A linear regression shows ~~a~~ reasonable concordance with R^2 = 0.95. Without windspeed corrections, *ME* is approximately 10-fold smaller than *RE*.

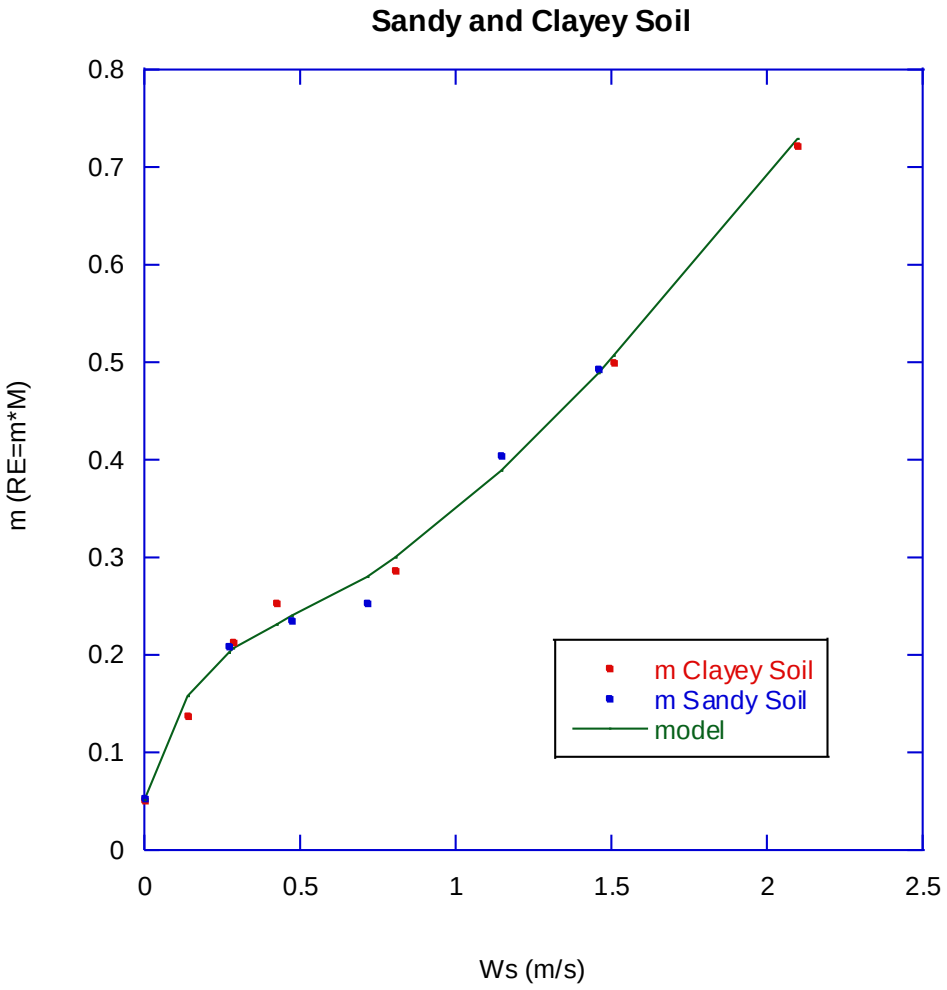

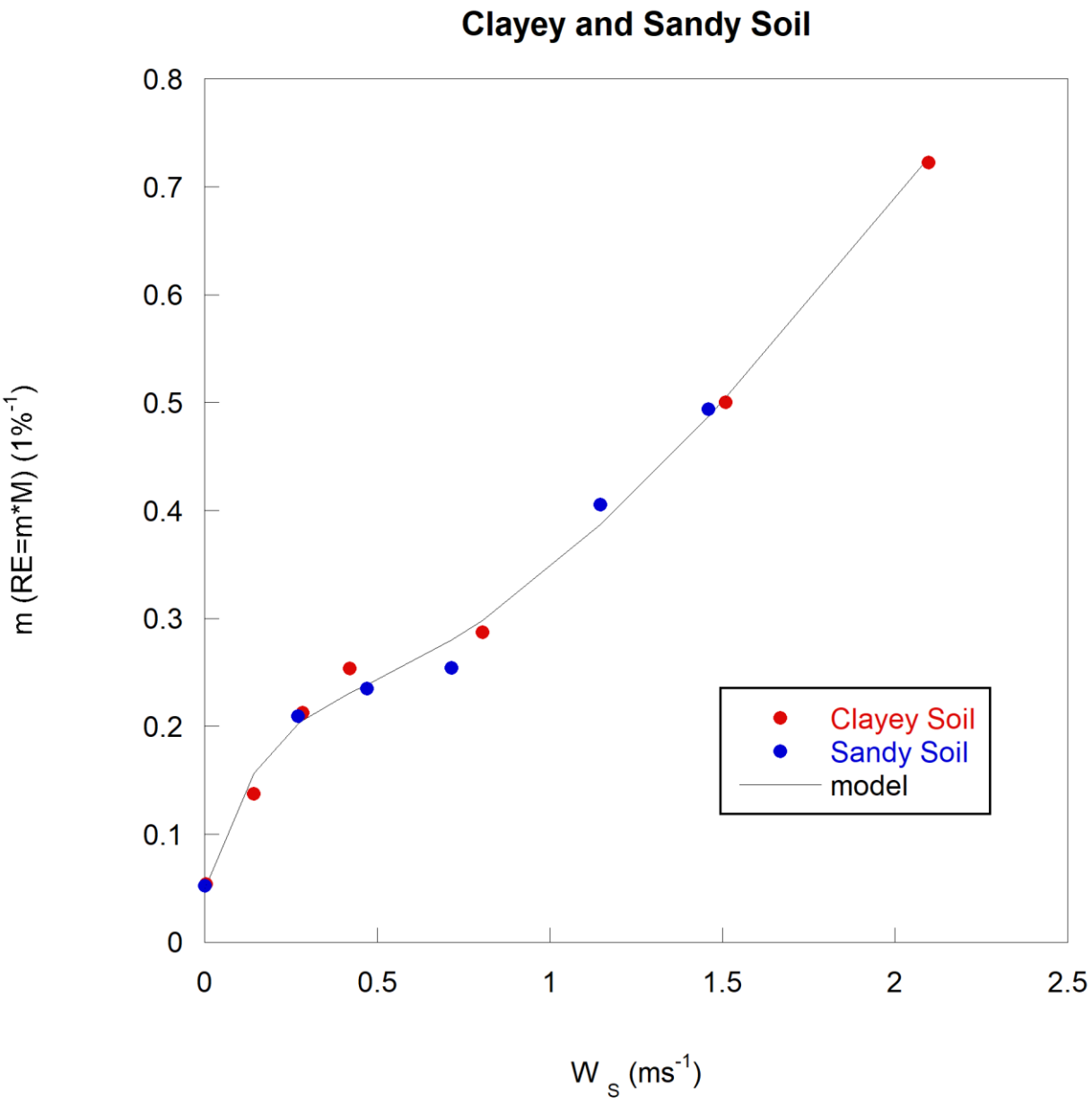

690 **Figure 07: *m* versus ~~gravimetric soil water content,~~wind speed~~s~~ for sandy soil and clayey soil.**

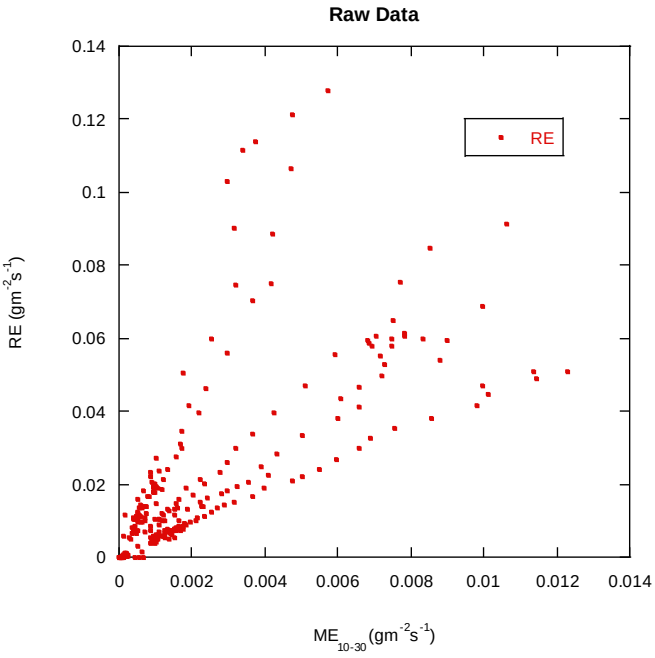
Raw Data
RE
RE (gm-2s-1)
ME10-30 (gm-2s-1)
0.14
0.12
0.1
0.08
0.06
0.04
0.02
0
0.002
0.004
0.006
0.008
0.01
0.012
0.014

a)

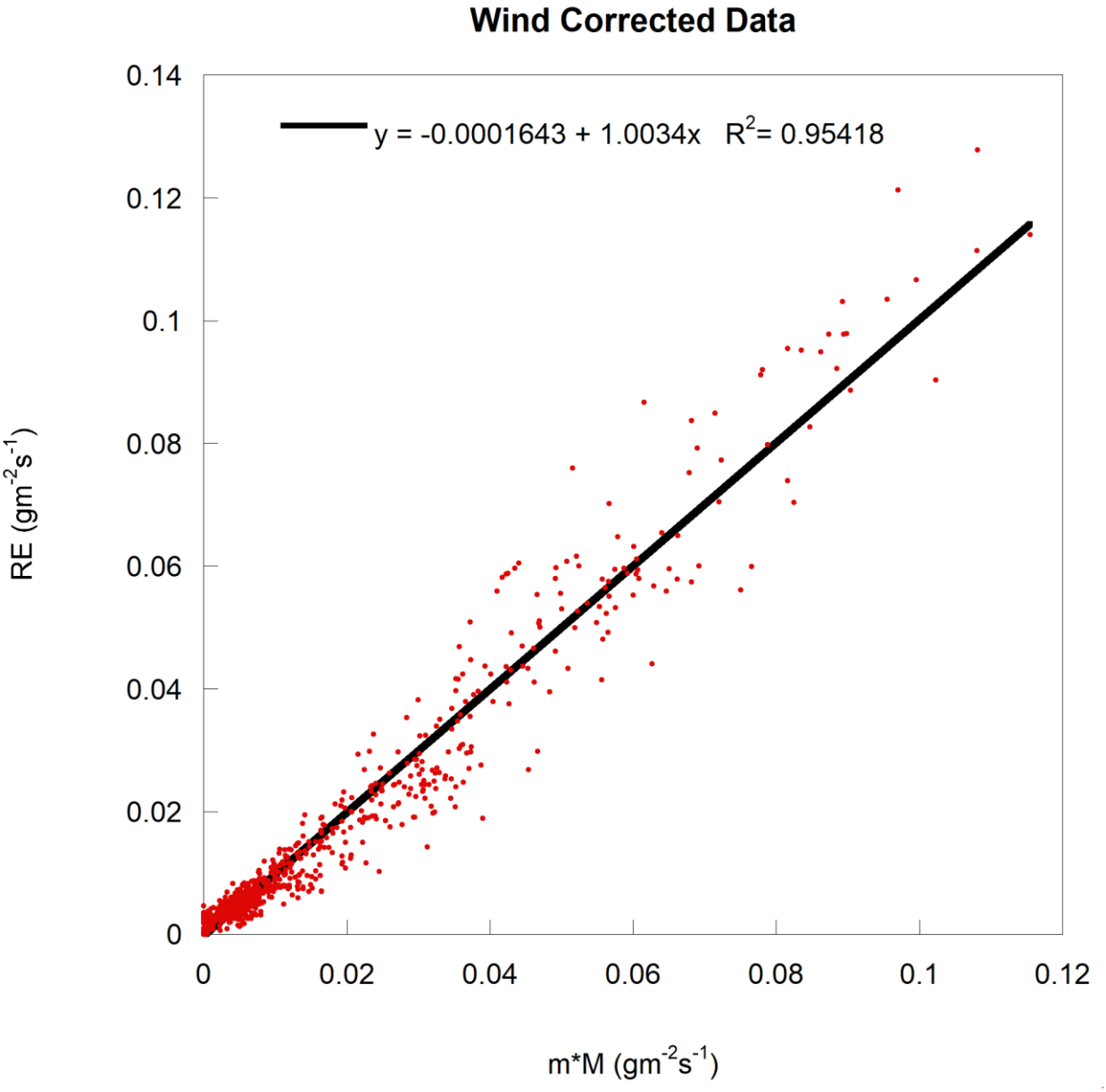
Wind Corrected Data
y = -0.0001643 + 1.0034x R2= 0.95418
RE (gm-2s-1)
m*M (gm-2s-1)
0.14
0.12
0.1
0.08
0.06
0.04
0.02
0
0
0.02
0.04
0.06
0.08
0.1
0.12

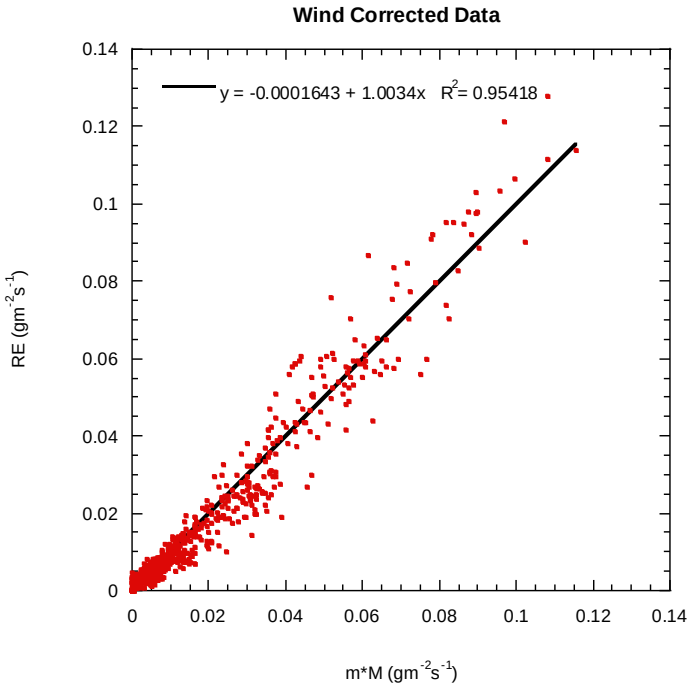

b)

Figure 08: ~~Real evaporation versus m~~***a) RE*** **versus** ***ME (raw data*****, average between PWM=10 and PWM=30% measurements).** ***b) RE*** **versus wind speed corrected** ***ME*** **for all disponible data along with a linear regression.**

~~4.3.2 Laboratory measured soil evaporation *ME* results~~

~~It is well known and admitted that the soil evaporation can be divided into three stages. (Introduced by Philip 1959, Wilsdon and al. 1994 or Hiller 2004). The wet soil, water saturated or near to water saturated, is evaporating with a constant rate greatly depending on the wind. With the progressively drying soil, a second stage appears after the so-called Air Entry Value (AEV) and shows a smallest wind dependence. A third stage is concerning the very dry soils with a constant extremely low evaporation rate and was not really observed in this study except the zero-wind sand evaporation record that took over two months of constant monitoring. In order to compare measurements under different wind speeds, such as the real evaporation from sandy and from clayey soils, a semi logarithmic scale versus soil moisture is probably the most relevant way Fig. 09. On these figures, we can notice that regarding the sand, the first stage is important comparatively to the clayey soil where the evaporation is quickly falling to the second stage. This behaviour is characteristic for a relatively low-rate evaporation on a sandy soil (Holmes 1961). The second stage displays a very linear behaviour for the sand and also for the clay on the logarithmic scale. This means that, in the second stage, the evaporation rate is as an exponential function of the soil moisture *w*.~~

$$RE_{Second\ Stage} = C(w_s) * e^{D*w}$$

~~(11)~~

~~With *C* depending slightly on the~~ Wind speed~~,~~ ~~w_s and *D* being a constant almost independent of the wind for a sandy soil.~~

~~**Indeed, regarding the sandy soil, whatever is the wind, the slopes are the same and the curves are parallel but remain slightly wind**~~ **affected** ~~**since they are not superimposed.**~~ ~~***ME***~~

This section describes the differences between *RE* and *ME* under a strong wind. Two phenomena were identified: water vapor sorption by wind-dried soil and inertial water vapor effluxes after chamber head deployment. Special attention should be given to clayey soils under changing wind and to the first 60 s of measurements after chamber head deployment.

4.3.1 Water vapor sorption

~~For the clayey soil, the second stage evaporation rates are higher for the higher wind.~~ ~~There is a well visible common point where the evaporation rates are the same whatever is the wind. For a lower moisture, the curves clearly diverge as the slopes are different.~~

~~The difference between a sandy soil and a clayey soil draying process is certainly affected by the micro and later macro desiccation crack apparitions in the clayey soils (Lau 1987, Morris et al. 1992, Kodikara 2002).~~ ~~These cracks may be considered as an effective soil/air interface surface increase and then an additive water vapor exchange which may significantly increase the evaporation rate under the wind (Nachshon et al. 2012).~~ ~~The other difference between theses soils is the grain seize difference and then the intergrain void space, and the resulting matric suction amplitude as discussed later in this paper.~~

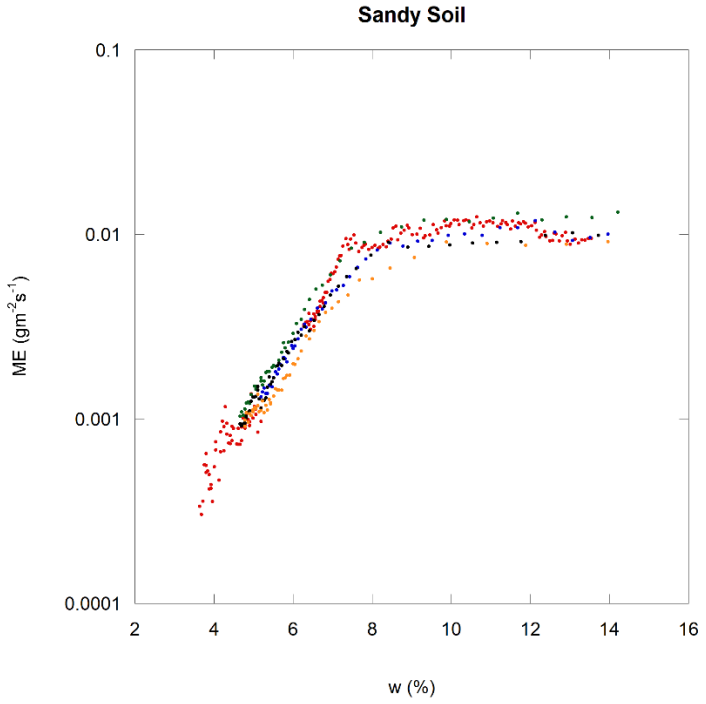

~~(a)~~

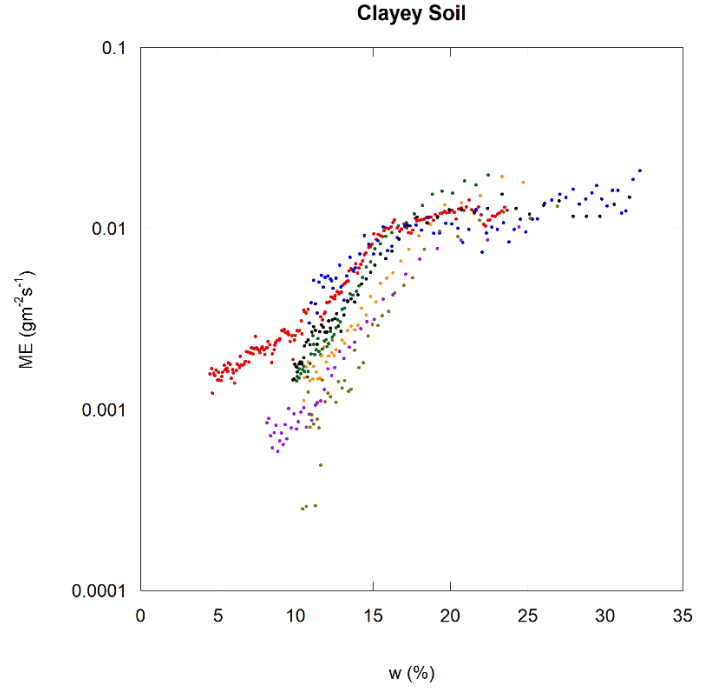

~~(b)~~

730 Figure ~~10: Measured Evaporation *ME* versus gravimetric soil moisture (PWM=30%); (a) for sandy soil and (b) for clayey soil for several wind speeds.~~

3.2.1 Wind affected measures *ME*

Figure 10 resumes09 shows the resumed *ME* versus the soil moisture for a sandy soil (a) and a clayey soil (b). For the sandy soil, as we can expect, since the measuresmeasurements are done under a chamber cloche that isolates the soil from the wind, the measures do not display a clear wind dependence. On the contraryIn contrast, for a clayey soil, converselyin contrast to the *RE*, *ME* decreases with the increasing wind speed. This finding may be explained by two facts:

ComparativelyCompared to the trace gas effluxeffluxes such as CO_2, CH_4 or N_2O effluxes, the water vapor efflux *RE* has two sources-sinks/source sink components: production (*P*) and stock (*S*) from the soil pores, by dissolution into the soil water or by sorption (absorption plus adsorption).

$$RE = P - \frac{\partial S}{\partial t} \tag{12}$$

Real surface efflux is then a result of the production less stock variation.

The wind may have a great influence on the efflux by forcing to unstock but much less or evereven nil influence on the production itself in the case of trace gases such as CO_2, N_2O or CH_4 and the deep subsurface evaporation with a low porosity soil.

In the case of a water vapor efflux, the soil water vapor stocking ability exists as well in the case of a dry soil layer formation (DSL) (E. Balugani et al., 2018) that concerns mainly the sandy soils under arid or semi-arid climatessemiarid climates (Wang, 2015), as in the case of a simply non-saturatednonsaturated soil (vadose zone) (Balugani et al., 2016)). In both cases the, stockage is realized in the soil pores saturated with the water vapor or by soil (mainly clay) sorption. The migration of the water vapor from this undersurface zone is the predominant *RE* process in the evaporation second stage (Geistlinger et al., 2018). Moreover, on the one hand, concerning the evaporation, the wind may directly influence directly the production in the shallow subsurface (Harris, 1916;; Smits, 2015;; a quasi-exhaustivequasiexhaustive list of the evaporationsevaporation factors is given by Faseel Suleman et al., 2017)), and, on the other hand, the soil is able to absorb the water vapor from a deeper and wetter evaporating soil layer or from the air, making the stock *S* dependent not only on the soil water vapor production *P* but also on the soil/atmosphere surface interaction (Amer, 2015). This last point may explain why the sandy soil chamber-based measurements are independent of the external wind when the clayey soil gives the measurements of the water vapor effluxes decreasing with the increasing external wind.

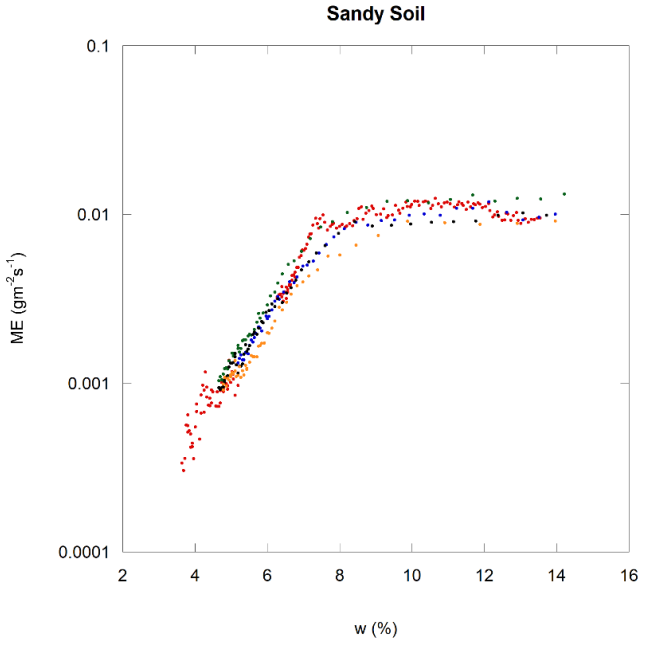

(a)

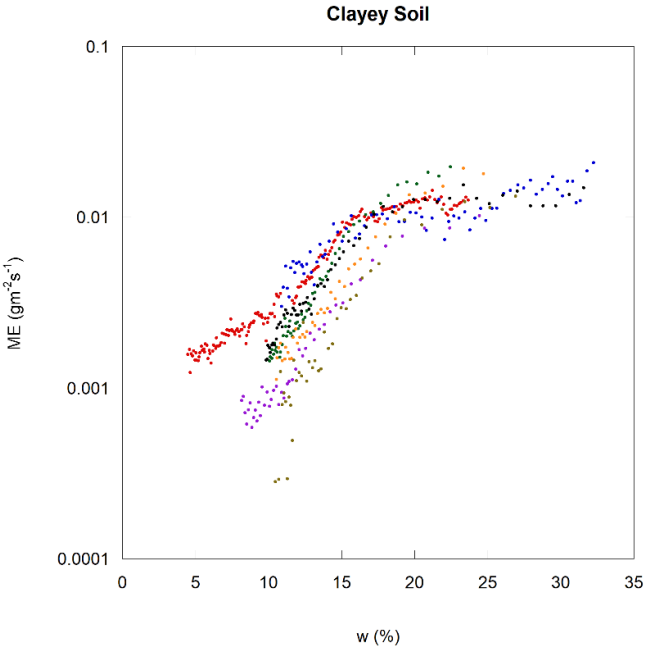

760 (b)

Figure 09: Measured evaporation *ME* versus gravimetric soil moisture (PWM=30%); (a) sandy soil, and (b) clayey soil at several wind speeds.

765 Indeed, the ~~soil~~ ability of soil to absorb water vapor ~~is increasing~~increases with ~~its particles size~~ decreasing particle size (Chiorean, 2017~~))~~, or~~,~~ by definition, ~~the~~ sand particles are ~~of a~~ several ~~magnitude bigger size~~magnitudes larger than ~~the~~ clay particles. ~~The~~ Sandy soil is then much less able to absorb water vapor ~~comparatively to the~~than clayey soil, for which ~~the~~ water vapor sorption is well known and documented from an experimental and theoretical point of view (Johansen and Dunning, 1957~~,~~; Likos and Lu, 2002~~,~~; Leelamanie, 2010 ~~or;~~ Arthur et al~~.~~., 2016). ~~In the~~Under windy conditions, the soil moisture top
770 ~~layers~~layer moisture is an equilibrium between ~~the~~ wind pumping and the soil water absorption/retention forces. When the wind ~~cease~~ceases, another equilibrium ~~has to~~must be reached with a ~~down~~lower soil layer of a higher moisture. ~~A~~ Short-term water vapor sorption by the previously wind-dried soil layer may significantly, but only temporarily, lower ~~down~~, the apparent evaporation rate *RE* (Jabro, 2009).

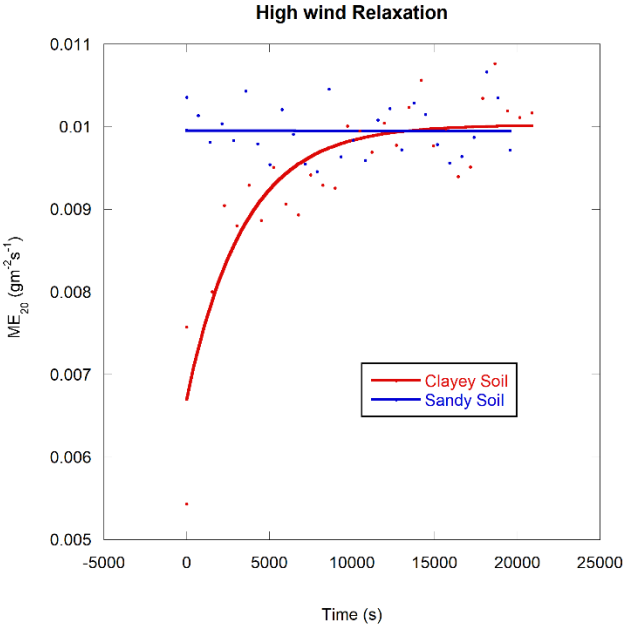

~~(a)~~

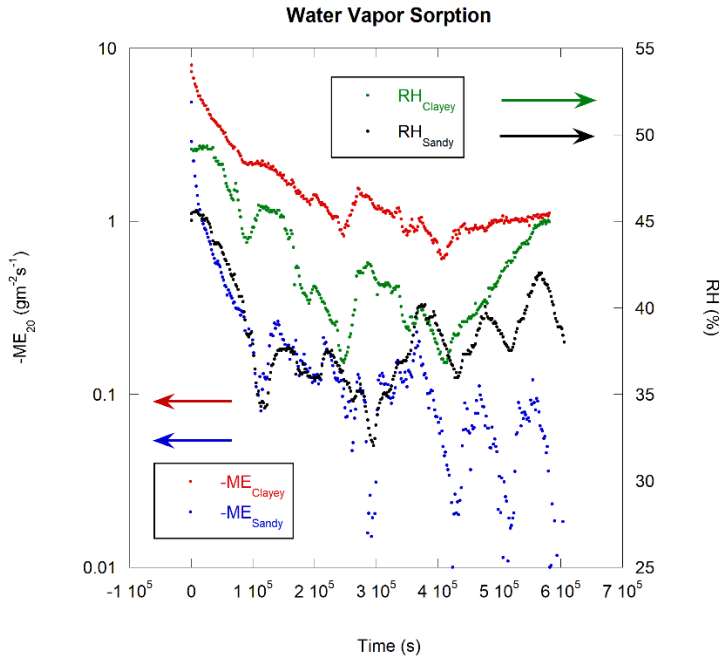

~~(b)~~

~~Figure 11: Measured (at PWM=20%) evaporation *ME* versus time (a) after a strong wind (W_S = 2ms^{-1}) for clayey and sandy soil. Slid line represents a linear regression~~ Consequently, *ME* behavior is very different for sandy soil and **~~an exponential regression~~** for clayey soil. **~~(b) after oven drying~~**When the chamber head is deployed, the external wind speed influence is stopped, and the internal fan influence is started. Sandy soil adapts almost immediately to the new conditions but not clayey soil. This point is important for **~~24H at 105°C~~**real measurements of clayey soil evaporation under changing wind speed, as the measured results correspond to the pondered integration of previous wind speed influences not only to the wind speed of the moment.

Figure ~~11~~10 (a) shows *ME* ~~behaviour~~behavior at always the same fan speed (*PWM* = 20%) over ~~a~~ wet sandy or clayey soil after one day of a strong wind that ceases immediately after the first measurement engagement (30 measurements, each chamber deployment ~~during~~for 10 minutes ~~inters spaced by~~interspersed with chamber opening and head space flushing ~~during~~for 1 minute).

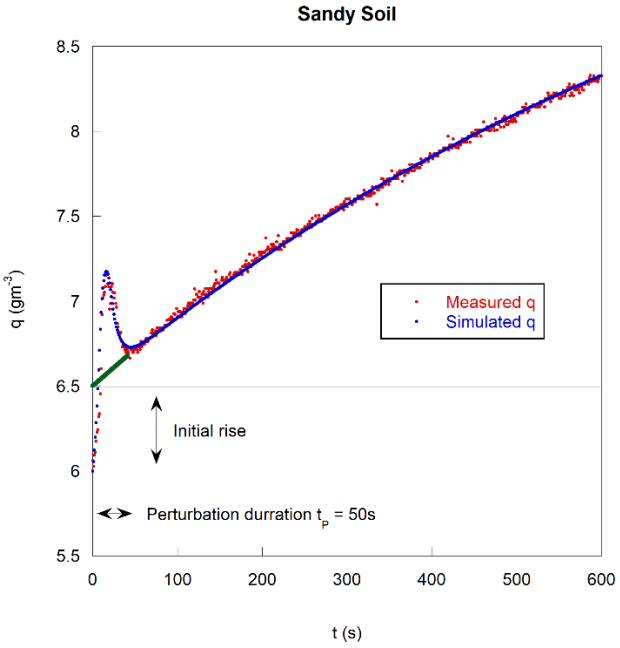

~~(a)~~

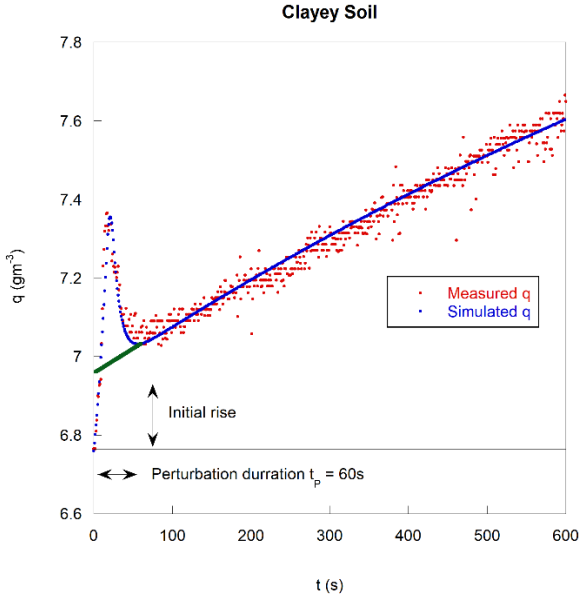

~~(b)~~

~~**Figure 12: Absolute water vapor concentration versus time. Measured concentration and simulated concentration, (a)**~~ For sandy soil ~~**and (b) clayey soil.**~~

~~**3.2.1.1 Inertia and chamber head air mixing time**~~

, the

~~During a chamber head deployment with a high-speed~~ wind ~~and a relatively wet sandy soil, an initial peak is observed in the enclosed air absolute humidity curve versus time (Fig. 12(a) for sandy soil and 12 (b) for clayey soil).~~

~~This is a direct consequence of a non instantaneous head space air mixing coupled with a high water vapor efflux in the boundary layer over the soil forced by the wind and is qualitatively well described by a very simple model of a mixed closed space air. A bigger volume of a low humidity air mixed with a smallest volume of a higher humidity air (boundary layer volume) intaking linearly is increasing humidity reaching a maximum and then is rapidly decreasing reaching a usual *ER* evolution (see the scheme on Fig. 13(a)). This mixing process may be described by an equation of the form:~~

$$C(t+dt) = a * C(t) + (1-a) * S(t)$$

~~(13)~~

~~With C(t) being the measured concentration of interest, a being the mixing ratio defined by the proportion of the recycled air divided by the proportion of the air coming from the boundary layer and S(t) being concentration within this layer. S(t) is a sum of a usual ER evolution $S_{ER}(t) = C_L - (C_L - C_S)*\exp(-t/\tau_0)$ with an overage of the water vapor due to the residue of a high wind forced efflux $S_R(t)$. This overage concentration is modelized starting from zero, reaching linearly a maximum value during about a half of the perturbation delay t_p and then decreasing quickly always linearly with time (Fig. 13(b)).~~

~~It reflects a boundary air layer of a high moisture, that is formed by a strong wind forced water vapor efflux, which is not immediately stopped by the chamber head closure (residual efflux). The resulting perturbation ceases after 50 seconds of the chamber head deployment for a sandy soil. This initial peak vanishes with a lower wind speed or a lower soil humidity or also a higher fan speed. For example, under PWM = 20%, the initial peak is hard to spot and is no more visible with the higher fan speeds whatever is the wind speed (in the studied range) or the soil humidity. The peak vanishes but an initial quick humidity rise inside the deployed chamber head is still visible.~~

~~Figure 12 displays, measured along a simulation, the resulting absolute water concentration inside the chamber head; (a) for a sandy soil and (b) for a clayey soil. Figure 13 provide the adjustment constants definitions. Additionally, we can understand:~~

- ~~C_0 as a starting concentration within the chamber head air (ambient concentration);~~
- ~~C_1 as the maximum concentration within the boundary layer due to the residual inertial efflux enrichment in competition with the chamber head enclosing the air mixing by the embedded fan;~~
- ~~C_S as the concentration resulting from the initial concentration raised by the residual inertial efflux (S_R is the residual surplus of the boundary concentration due only to the residual inertial contribution), a is the fan mixing ratio, t_m is the residual efflux duration, t_e time of the residual efflux duration enhanced by the effective mixing time (13s in our case), τ_0 resulting characteristic time for an *ER* concentration evolution; and~~
- ~~C_L is the concentration of the boundary layer but on the soil side (limit of the concentration within the deployed chamber head after an infinite duration).~~

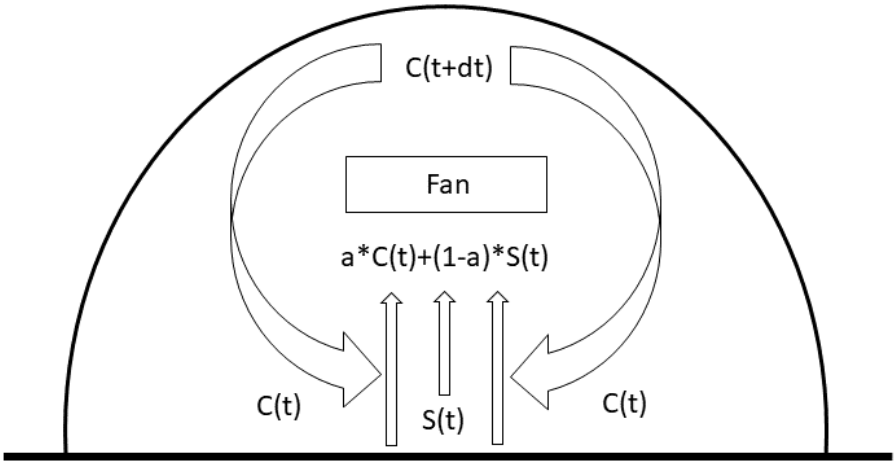

~~(a)~~

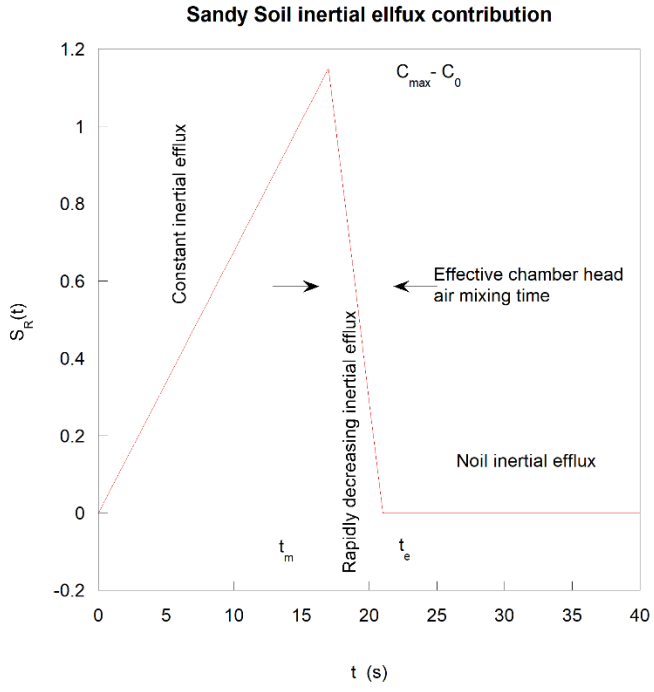

~~(b)~~

~~Figure 13: (a) Chamber head air mixing principle. (b) Residual water vapor efflux to the boundary layer water vapor concentration S_R versus time.~~

~~Indeed, the same measurement (PWM=10% under a high wind and a soil moisture) performed with a clayey soil (Fig. 12(b)) shows also an initial peak but, comparatively to the sandy soil (Fig. 12(a)), this peak, as the whole evaporation rate, is of a~~

~~smallest amplitude since the water vapor efflux, as discussed previously, is absorbed by the top soil layer initially dried by the wind pumping. With a clayey soil, the initial peak perturbation duration is also slightly longer (60s) comparatively to a sandy soil (50s).~~

~~This initial peak requires a special attention during the *ER* regression calculations in order to do not bias the results. An initial short time laps exclusion, 50s-60s in this case, may be necessary. The data points should be discarded but it is important to do not change the time origin because it may lead to an important flux calculation bias (5% in this sandy soil case). The amount of the water vapor released during first 50s is rising significantly the initial water vapor concentration measurements and the total water vapor content inside the chamber head (initial rise), but does not impact further efflux calculations.~~

~~For both simulations, the constants tied with the chamber design such as a = 0.9 and effective mixing time t_e-t_m = 13s, are the same and only constants tied with the soil samples nature change.~~

~~Sandy soil: C_0 = 6 g/m^3, C_1 = 1.35 g/m^3, C_S = 6.55 g/m^3, C_L = 9.7 g/m^3, t_e = 21s, t_m = 8s, τ_0 = 900s.~~

~~Clayey soil: C_0 = 6.76 g/m^3, C_1 = 0.8 g/m^3, C_S = 6.96 g/m^3, C_L = 8.74 g/m^3, t_e = 30s, t_m =17s, τ_0 = 1500s.~~

~~Comparatively to the sandy soil, the residual efflux due to the wind is of a smallest amplitude but longer.~~

~~3.2.1.2 ME: results for sandy soil~~

~~The wind is drying~~dries the soil sample, but ~~the~~ chamber deployment, even if it insulates the soil sample from the external wind, does not give an opportunity to the shallow, wind-dried~~,~~ layer of ~~a~~ sandy soil to reabsorb water vapor from the air or from the deeper soil~~,~~ and does not limit the measured evaporation rate (Figure 10). ~~It is worth to be noted that~~ For both~~, the~~ sandy soil and ~~the~~ clayey soil, the difference ~~of the~~in real evaporation is ~~about~~approximately one decade between ~~a~~ zero-wind evaporation and ~~a~~ small-wind evaporation~~. This~~, which can be attributed to a shallow boundary air layer over the soil that is disturbed by any wind. Without ~~the~~ wind, this boundary has a high -water vapor content, limiting ~~the~~ evaporation from the soil by molecular diffusion. A slow advection is also present (water vapor is lighter than the air~~)~~), but this transport is visibly very slow.

~~3.2.1.3 ME: results~~ For clayey soil, the wind ~~is drying~~dries the soil sample in the same way as for the sandy soil. However, after ~~the~~ chamber deployment, a previously wind-~~drayed~~-dried clayey soil layer ~~is absorbing the~~absorbs water vapor from the deeper wetter soil, reducing the net water vapor efflux *ME*. The measured surface efflux is real, but the conditions are not. We are in a transition regime caused by ~~the~~ chamber deployment and the measured soil portion isolation from the external wind. In the sandy soil case, this transition period is very short (*ME* is wind independent) and does not affect the measurement when, in the case of a clayey soil, this transition period is long and the characteristic time deduced from an exponential rise regression is ~~about~~approximately one hour long. The clayey soil sample needs ~~about~~approximately four hours to reach equilibrium ~~from~~ under a wind speed ~~(~~*Ws*~~) *Ws* = 2ms~~ = 2 ms^{-1} to new equilibrium under a ~~*Ws* ≈ 0ms^{-1}~~nil wind speed *Ws* ≈ 0 ms^{-1}.

Figure ~~11~~10 (b) displays the *ME* ~~behaviour~~behavior at PWM=20~~%~~%, but this time, the soil sample was oven-dried for ~~24H~~24 h at 105 °C. The bucket with dried soil samples ~~were~~was sealed and opened just before the first measurement. ~~As we can see, both,~~Both the clayey soil and the sandy soil ~~are sorbing~~sorb the water vapor from the atmosphere (negative *ME*~~)~~), but the sandy soil sorption ~~is~~ quickly ~~falling~~falls to nearly zero when ~~the~~ clayey soil sorption is ~~perduring~~enduring and is inversely proportional to the air water demand.

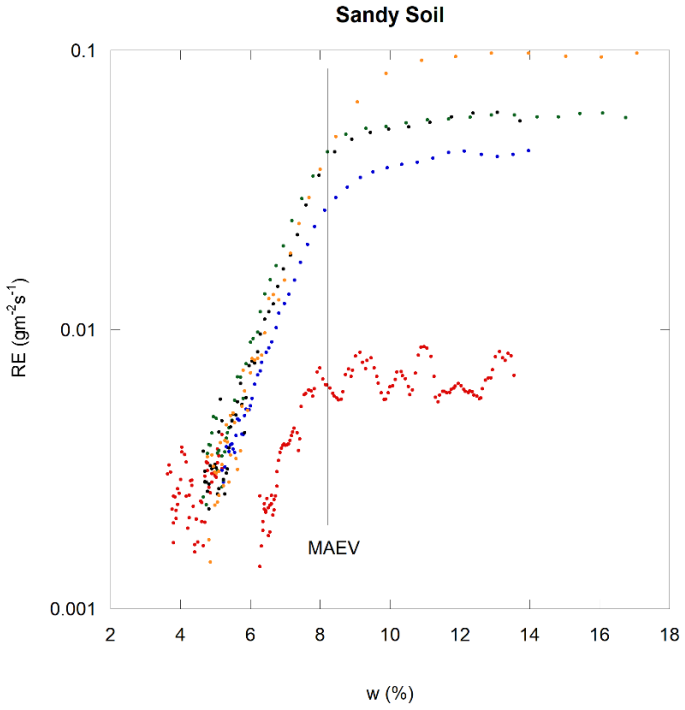
Sandy Soil
0.1
0.01
0.001
RE (gm-2s-1)
MAEV
2
4
6
8
10
12
14
16
18
w (%)

(a)

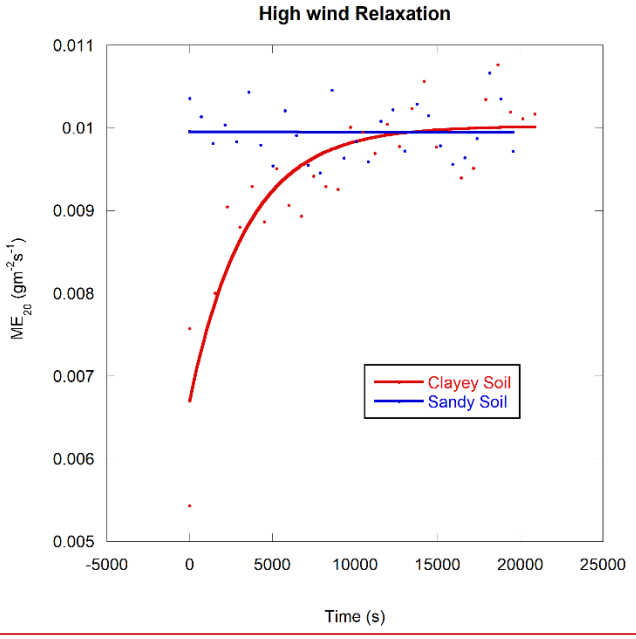
High wind Relaxation
0.011
0.01
0.009
0.008
0.007
0.006
0.005
ME20 (gm-2s-1)
Clayey Soil
Sandy Soil
-5000
0
5000
10000
15000
20000
25000
Time (s)

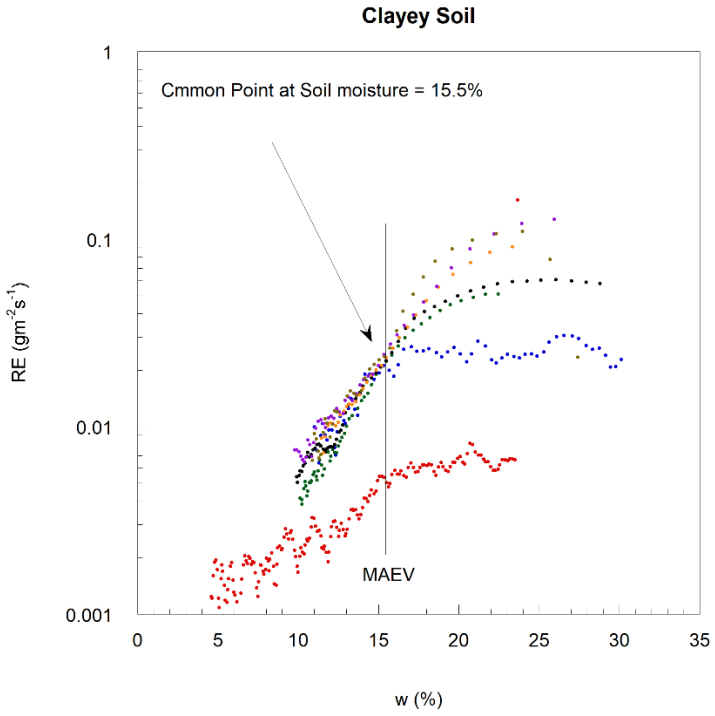
Clayey Soil
Cmmon Point at Soil moisture = 15.5%
MAEV
RE (gm-2 s-1)
w (%)
1
0.1
0.01
0.001
0
5
10
15
20
25
30
35

(b)

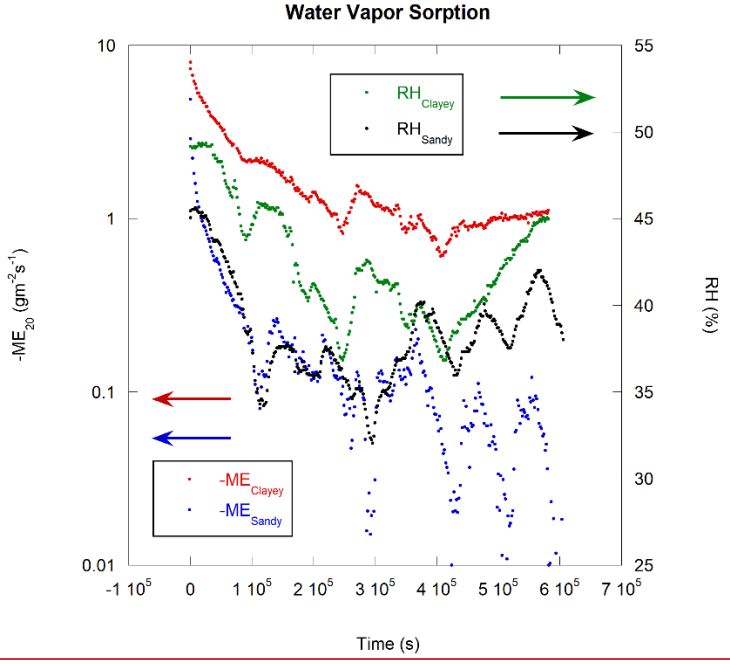
Water Vapor Sorption
RHClayey
RHSandy
-MEClayey
-MESandy
-ME20 (gm-2 s-1)
RH (%)
Time (s)
10
1
0.1
0.01
55
50
45
40
35
30
25
-1 10^5
0
1 10^5
2 10^5
3 10^5
4 10^5
5 10^5
6 10^5
7 10^5

875

Figure ~~09: Real~~10: Measured (at PWM=20%) evaporation *ME* versus ~~gravimetric soil moisture~~ time (a) after a strong wind (W_S = 2 ms^{-1}) for clayey and sandy soil. The slide line represents a linear regression for sandy soil and ~~b)~~ an exponential rise regression for clayey soil ~~for several wind speeds.~~

880

~~3.2.2 Real Evaporation *RE* of clayey soil~~

~~3.2.2.1 Soil cracking~~

~~The cracks formation in a~~**. (b) after oven drying** ~~clayey soil, also called desiccation soil cracks, has a great influence on the total evaporation up to 50% enhancement according to Hatano et al. (1988) and, under the windy condition, the total~~
885 ~~evaporation may be even increased by two orders of magnitude (Nachshon et all. 2012). This phenomenon is widely studied and relatively well documented as its consequences~~ **for** ~~the engineering (Lytton et al. 1976, Daniel et al 1993, Kodikara et al. 2002, Rodriguez et al. 2007, Stirling et al. 2017) and the agriculture (Pal et al. 2012, Kurtzman et al. 2016) are very important. Picture 14 shows the clayey soil sample in its dry state; (a) dried under a moderate wind, (b) dried under no wind. During this study, different cracks patterns are obtained with a different wind speed and a different drying ratio. An obvious wind~~
890 ~~importance on the cracking pattern was noticed. Higher is the wind more numerous are the cracks in accordance with existing studies (Corte and Higashi 1960, Tang et al. 2008 and 2010, Costa et al. 2013) and coarsest are the resulting cracks pattern always in accordance with the previous studies (Corte and Higashi 1960, Lau 1987, Kodikara et al. 2000, Nahlawi and Kodikara 2006, Tang et al. 2008 and 2010, Costa et al. 2013), due to an important matric suction increase with the drying ratio in a clayey soil. This is a part of so-called *dynamic effects*. The studied clayey soil sample can lose up to 15% of its initial~~
895 ~~volume and its observation drying under different winds speeds allows to point out an interesting finding which is an existence of a common point (*CP*) and a change in the evaporation ratio versus soil moisture slope below this point under all wind speeds but nil. The clayey soil sample is cracking under the wind but is drying as a whole block without cracks under the nil wind (Fig. 12(b)) creating a void space between the soil block and the bucket wall~~**24 h at 105 °C.**

~~*CP* corresponds to a well-defined and constant *RE* about 0.024 gm^{-2}s at a constant soil moisture *w* about 15.5%. It corresponds~~
900 ~~also to the *RE* versus *w* slope change for a drying soil. At the current research advancement point, one can only propose a hypothesis to explain this phenomenon tied with the clayey soil Matrix air Entry Value (MAEV) corresponding to the air seepage through the soil matrix, but the present study does not allow to prove it. Soil *RE* is slowing down with the soil moisture decrease, however, in the swelling clayey soil case, the soil moisture decreases cause also micro-cracks and hollows formation, depending on the expansive clay content (smectite minerals, including montmorillonite and bentonite) and more precisely its~~
905 ~~vertisol character (Ahamad 1996, Everest et al. 2016), increasing effective soil/atmosphere interaction surface (Bronswijk 1988).~~

(a)

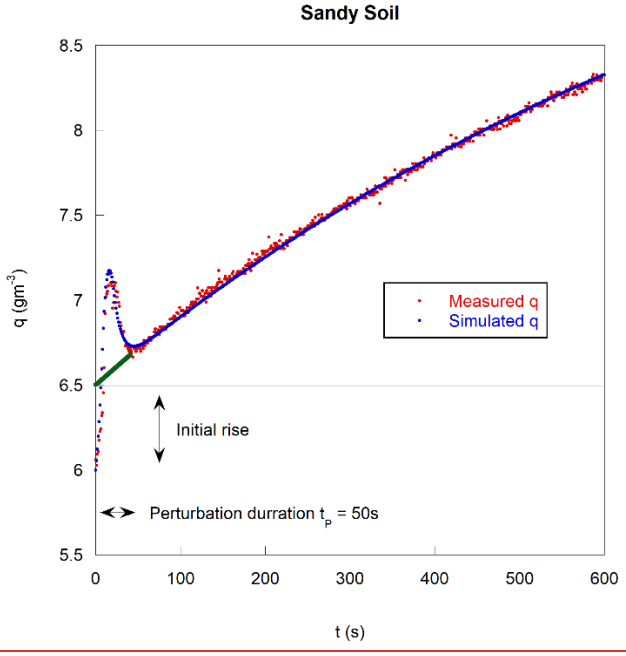
Sandy Soil
8.5
8
7.5
7
6.5
6
5.5
q (gm^{-3})
0
100
200
300
400
500
600
t (s)
Measured q
Simulated q
Initial rise
Perturbation durration t_P = 50s

910 (a)

(b)

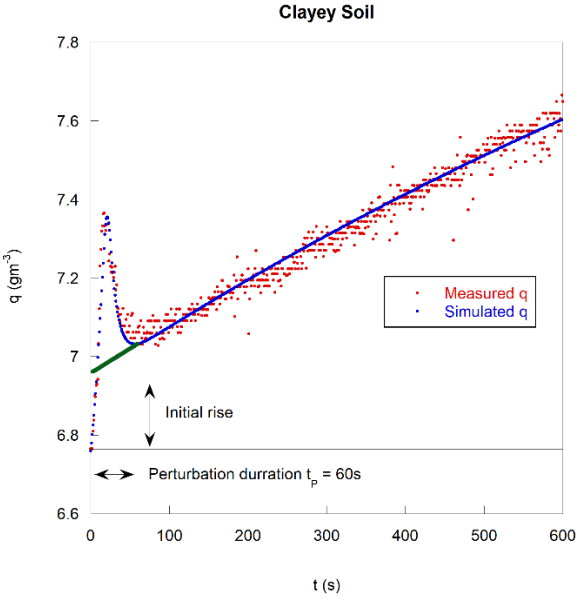

Figure ~~**14: Dried clayey soil surface after drying under (a) moderate wind of 0.8ms^{-1} (b) no wind.**~~

915 ~~This fact agrees with a relatively less pronounced transition between the first and the second stage of the evaporation observed in a clayey soil~~**11: Absolute water vapor concentration versus** ~~a~~ **time. Measured concentration and simulated concentration: (a) sandy soil** ~~(Fig. 09). As the wind influence importance on the *RE* goes together with the interaction surface, any change in the later is visible in the former. The cracks formation in the soil would increase *RE* changing the *RE* versus w~~

~~ratio~~ **, and** ~~may then explain the apparent slope change observed in the Fig. 09 (b). However, the cracks transform the soil sample to a fractured media, and are visible well before the *CP* point as showed by Song et al. 2016, cracking are forming a so called Cracking Air Entry Value (CAEV) on a moistest, almost saturated, clayey soil and their formation is progressive which is rather incompatible with a brusque slope change. The concerned soil moisture point *CP* seems to correspond rather to a soil matrix air entry value (Azam et al. 2013) below which the soil is acting as a porous media. The crack formation causing the first *AEV (CAEV)* on a soil moisture characteristic curve is followed by the matrix *AEV* (MAEV) formation on a drier soil and is very similar to a bimodal grain-size distribution curve (Satyanaga et al. 2013) where both grains of big and small sizes are present in the soil with then two intergrains void space sizes. These two points: cracks and matrix AEV, happen in a draying clayey under the wind before the final Void Ratio stabilization (Péron and Laloui 2005) and affect an evaporation ratio which is one order of magnitude bigger than those of no wind evaporation. Since, under no wind, the CP is not visible, one can deduce that the cracks or/and the wind presence is necessary for it~~**(b) clayey soil.**

4.3.2 Soil evaporation inertia and chamber head air mixing time.

During chamber head deployment with a high-speed wind and a relatively wet soil, an initial peak is observed in the enclosed air absolute humidity curve versus time (Fig. 11(a) for sandy soil and 11 (b) for clayey soil).

This observation is a direct consequence of noninstantaneous head space air mixing coupled with a high-water vapor efflux in the boundary layer over the soil forced by the wind and is qualitatively well described by a very simple model of mixed closed space air. A larger volume of low-humidity air (chamber head) mixed with the smallest volume of high-humidity air (boundary layer volume) taken linearly increases the humidity, reaching a maximum, and then rapidly decreasing, reaching a usual *ER* evolution (see the scheme in Fig. 13(a)). This mixing process may be described by the following equation:

$$C(t+dt) = a * C(t) + (1-a) * S(t) \quad (13)$$

where C(t) is the measured concentration of interest, a is the mixing ratio defined by the proportion of the recycled air divided by the proportion of the air coming from the boundary layer and S(t) is the concentration within this layer. S(t) is the sum of the usual ER evolution $SER(t) = C_L - (C_L - C_S) * exp(-t/\tau_0)$ with an overage of the water vapor due to the residue of a high wind forced efflux $S_R(t)$. This overage concentration is modeled starting from zero, reaching a linear maximum value during approximately half of the perturbation delay t_P and then decreasing quickly and always linearly over time (Fig. 12(b)). This process reflects a boundary air layer of high moisture that is formed by a strong wind-forced water vapor efflux, which is not immediately stopped by chamber head closure (residual efflux). The resulting perturbation ceases after 50 seconds of chamber head deployment for sandy soil. This initial peak vanishes with a lower wind speed, a lower soil humidity or a higher

fan speed. For example, under PWM = 20%, the initial peak is hard to spot and is no longer visible with higher fan speeds regardless of the wind speed (in the studied range) or the soil humidity. The peak vanishes, but an initial quick humidity rise inside the deployed chamber head is still visible.

Figure 11 also displays a simulation of the resulting absolute water concentration inside the chamber head; (a) for sandy soil, and (b) for clayey soil. Figure 12 provides the adjustment constants definitions:

- C_0 is the starting concentration within the chamber head air (ambient concentration).
- C_1 is the maximum concentration within the air boundary layer due to the residual inertial efflux enrichment in competition with the chamber head enclosing the air mixing by the embedded fan.
- C_S is the concentration resulting from the initial concentration raised by the residual inertial efflux (S_R is the residual surplus of the boundary concentration due only to the residual inertial contribution), a is the fan mixing ratio, t_m is the residual efflux duration, t_e time of the residual efflux duration enhanced by the effective mixing time (13s in our case), τ_0 is the resulting characteristic time for an *ER* concentration evolution.
- C_L is the concentration of the boundary layer but on the soil side (limit of the concentration within the deployed chamber head after an infinite duration).

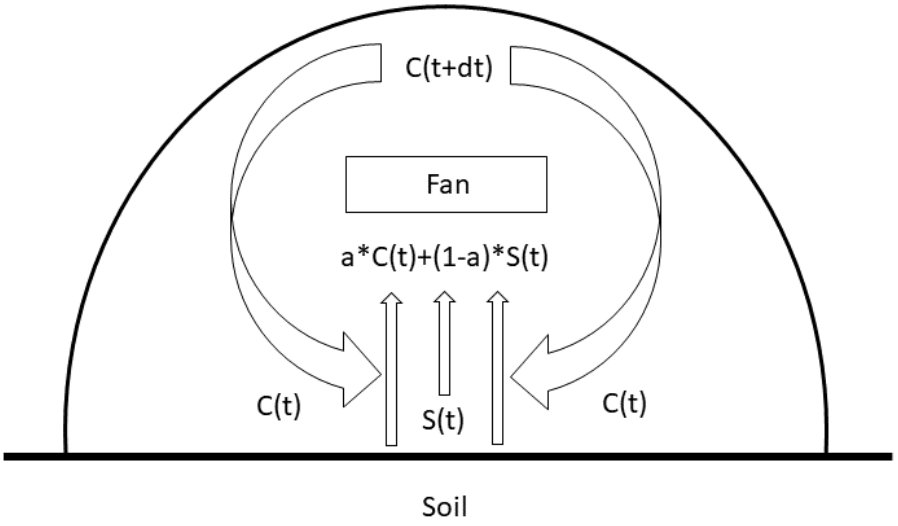

(a)

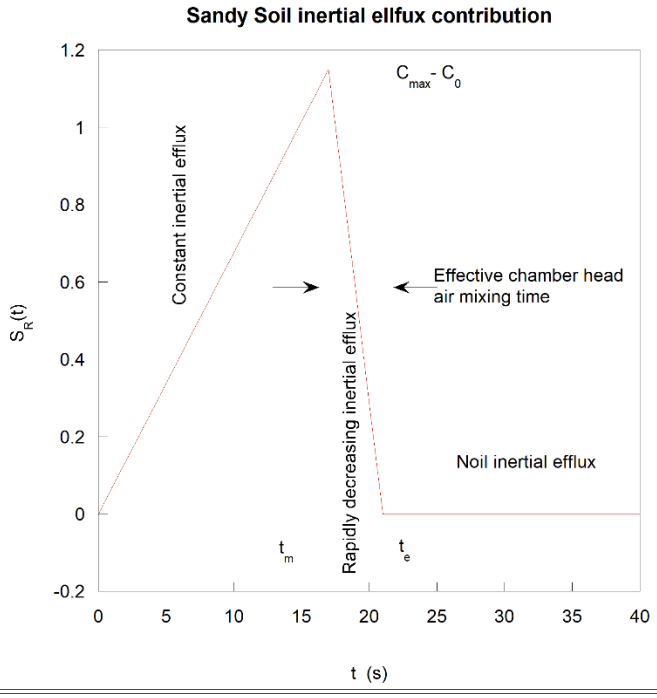

(b)

Figure 12: (a) Chamber head air mixing principle. (b) Residual water vapor efflux to the boundary layer water vapor concentration S_R versus time.

Indeed, the same measurement (PWM=10% under a high wind and ~~**Conclusion.**~~ soil moisture) performed with clayey soil (Fig. 11(b)) also shows an initial peak, but compared to sandy soil (Fig. 11(a)), this peak, as the whole evaporation rate, is of the smallest amplitude since the water vapor efflux, as discussed previously, is absorbed by the topsoil layer initially dried by wind pumping. With clayey soil, the initial peak perturbation duration is also slightly longer (60 s) than the initial peak perturbatioin of sandy soil (50 s).

This initial peak requires special attention during the *ER* regression calculations to avoid biased results. An initial short time lap exclusion, 50 s-60 s in this case, may be necessary. The data points should be discarded, but it is important not to shift the time origin because it may lead to an important flux calculation bias (5% in this sandy soil case). The amount of water vapor released during the first 50 s significantly increases the initial water vapor concentration measurements and the total water vapor content inside the chamber head (initial rise) but does not impact further efflux calculations.

For both simulations, the constants tied to the chamber design, such as a = 0.9 and effective mixing time t_e-t_m = 13 s, are the same, and only constants tied to the soil sample composition change (Table 1).

	C_l (g.m^{-3})	C_0 (g.m^{-3})	C_S (g.m^{-3})		C_L (g.m^{-3})	t_e (s)	t_m (s)	τ_0 (s)
Sandy soil	6	1.35	6.55		9.7	21	8	900
Clayey soil	6.76	0.8	6.96		8.74	30	17	1500

(1)

Compared to sandy soil, the residual efflux due to wind has the smallest amplitude but is longer.

Conclusions

The aim of these studies was to build a self-calibrating chamber based on an NSS technique and a simple working protocol to correct the measured data versus the wind. The proposed chamber design along with a deployment and correction protocol allow aallows $R^2 = 0.95$ confidence on a sandy or clayey bare soil andfor the surface wind in the range of 0 to 2ms2 ms^{-1}. The correction function has only one variable; the wind speed (measured a few centimetrescentimeters above the soil surface) regardless of any other parameter, such as soil naturecomposition, soil texture, soil temperature or meteorological variable. However, a study of the higher wind speeds is suitable but exceeds the ability of the present experimental set upsetup. The presented results are valid for a bare soil chamber-based measurement. In the vegetatedvegetative plot case, the measured wind speed onat the chamber level will be comparatively slow-; however, the wind influence is still important and forced below the canopy wind speed through the eddy pressure fluctuations (Kimball and Lemon, 1970-1971-; Baldocchi and Meyers, 1991-; Takle et al-., 2004-; Maier et al-., 2010-; Mohr et al-., 2016-; Poulsen et al-., 2017-; Mohr et al-., 2017). The wind eddy pressure fluctuations generated by the above canopy penetrate below the canopy, forcing the soil gasesgas efflux. This is a so-called pressure pumping that may be responsible ofor up to 50- to 100-fold enhanced effluxes. In other words, the most relevant way to correct the chamber-based measurements below the canopy is to correct it with the pressure fluctuationsfluctuation power spectrum or a pressure pumping coefficient (PPC) defined by Mohr et al-., 2017 measured onat the soil level. However, for the bare soil, such as PPC, and the corelatedcorrelated wind speed, without the presence of vegetation presence, wind speed measurements remain valid for the chamber-based measurementsmeasurement correction.

An important experimental campaign concerning CO_2 effluxes measured by the NSS technique is currently in progress, and the first results are showing that described methodology (several consecutives'consecutive measurements with a different fan speed in order to deduce real efflux) is not directly applicable to other gases effluxesgas efflux measurements by the NSS technique such as CO_2 or N_2O, probably because, contrary to the evaporation, the wind speed is acting mainly acting on the stock and not on the production of these gases. However, a similar technique is not excluded.

During the calibration measurements, some interesting observations concerning the sandy soil evaporation process and chiefly clayey soil evaporation process are reported.

All the soil samples under all the studied winds display two evaporation stages~~,~~: the first ~~one~~stage is almost constant with ~~a~~ lowering soil moisture and is greatly affected by ~~the~~ wind, and the second ~~one~~stage is less affected by ~~the~~ wind with ~~an~~ exponential ~~behaviour~~behavior versus ~~the~~ soil moisture. These two evaporation stages are well described by *Z* variations, which are higher in the first stage. Both soil samples display a decade of *RE* difference without the wind and with a very small wind due to the air boundary layer perturbation.

~~The~~ Sandy soil does not display ~~an observable~~a consequent ability to absorb ~~the~~ water vapor, and its stocking capacities are limited. However, the apparent evaporation inertia is ~~well~~ conspicuous on the relatively wet soil under a relatively strong wind. ~~The~~In contrast, clayey soil~~, on the contrary,~~ displays a great sorption ability and water vapor stocking or unstocking capacities with a characteristic time in the ~~hour~~hourly range. The inertia is partially screened by the sorption magnitude, and a strong external wind is necessary. As described in Appendix A, in the second soil evaporation stage, regardless of the soil, evaporation follows an exponential law versus *w*. In clayey soil, the evaporation curve versus ~~soil water content~~SWC *w* shows a common point *CP* (*w* = 15.5% and *RE* = 0.~~024gm~~024 $gm^{-2}s^{-1}$) for every wind and soil ~~textures~~texture but a nil wind speed. The curve evaporation versus water content below the *CP* ~~change~~changes its slope. This point seems to correspond to the matrix air entry value (MAEV~~,~~).

Competing interests. The author declare that ~~they have~~he has no conflict of interest.

Acknowledgements. This study was mainly funded by ICOS France and Anna Zawilski (private donations). I would like to acknowledge Tiphaine Tallec (CESBIO, Toulouse, France) for her useful discussions. A special thanks to Valérie Le Dantec (CESBIO, Toulouse, France) who greatly contributed to motivate this work. I am particularly grateful to Katia Bonne (LI-COR Biosciences GmbH, Bad Homburg, Germany) and Jason Hupp (LI-COR Biosciences, Nebraska, USA) for discussions and communications.

References

Ahamad, N~~.,~~.: Occurrence of distribution of Vertisols. In: Ahmad, N., Mermut, A. (eds.) Vertisols and Technologies for their Management, Development in Soil Science, 24: 1–41, doi:10.1016/S0166-2481(96)80003-1, 1996.

Amer, A. M~~. A.,~~.: Water Vapor Adsorption and Soil Wetting, Chapter 1, https://www.intechopen.com/books/wetting-and-wettability, doi:10.5772/60953, 2015.

Arthur, E., ~~M.~~ Tuller, ~~P.~~M., Moldrup, P., and ~~L. W~~. de Jonge, L. W: Evaluation of theoretical and empirical water vapor sorption isotherm models for soils, Water Resour. Res., 52, 190–205, doi:10.1002/2015WR017681, 2016.

Aubinet, M., ~~T.~~ Vesala, ~~D.~~T., Papale, D.: Eddy Covariance, A Practical Guide to Measurement and Data Analysis, Springer Dordrecht Heidelberg London New York, doi:10.1007/978-94-007-2351-1, 2012.

Bain, W. G., ~~L.~~ Hutyra, ~~D.C.~~L., Patterson, ~~A. V.~~D. C., Bright, ~~B. C.~~A. V., Daube, ~~J. W.~~B. C., Munger, ~~S.C.~~J. W., Wofsy, S.C.: Wind-induced error in the measurement of soil respiration using closed dynamic chambers, Agricultural and Forest Meteorology, 131 225–232, doi:10.1016/j.agrformet.2005.06.004, 2005.

Baldocchi, D. and ~~T.~~ Meyers, T.: Trace gas exchange above the floor of a deciduous forest: 1. Evaporation and CO2 efflux, Journal of Geophysical Research Atmospheres, 96(D4):7271-7285, doi:10.1029/91JD00269, 1991.

Balugani, E., ~~M. W.~~ Lubczynski, ~~K.~~M. W., and Metselaar, K.: A framework for sourcing of evaporation between saturated and unsaturated zone in bare soil condition, Hydrological Sciences Journal – Journal des Sciences Hydrologiques, VOL. 61, NO. 11, 1981–1995, doi:10.1080/02626667.2014.966718, 2016.

Balugani, E., ~~M. W.~~ Lubczynski, ~~C.~~M. W., van der Tol, ~~K.~~C., Metselaar, K.: Testing three approaches to estimate soil evaporation through a dry soil layer in a semi-arid area, Journal of Hydrology, 567 405–419, doi:10.1016/j.jhydrol.2018.10.018, 2018.

Bornemann, F~~.~~,.: Kohlensaure und Pflanzenwachstum. Mitt. Dtsch. Landwirtsch-Ges. 35:363, 1920.

Brændholt, A., ~~K.~~ Steenberg Larsen, ~~A.~~K., Ibrom, ~~K.~~A., and Pilegaard, K.: Overestimation of closed-chamber soil CO2 effluxes at low atmospheric turbulence, Biogeosciences, 14, 1603–1616, doi:10.5194/bg-14-1603-2017, 2017.

Bronswijk, J. J. B~~.~~,.: Modeling of water balance, cracking and subsidence of clay soils, Journal of Hydrology February 1988, Volume 97, Issues 3–4, 15, 199-212, doi:10.1016/0022-1694(88)90115-1, 1988.

Chiorean, V-F~~.~~,.: Determination of Matric Suction and Saturation Degree for Unsaturated Soils, Comparative Study - Numerical Method versus Analytical Method, 2017 IOP Conf. Ser.: Mater. Sci. Eng. 245 032074, doi:10.1088/1757-899X/245/3/032074

Chung, E-S., ~~B.~~ Soden, B~~. J.~~., Sohnb, B. J., and L. Shic~~.~~: Upper-tropospheric moistening in response to anthropogenic warming, PNAS (2014), vol. 111, no. 32, 11636–11641, doi:10.1073/pnas.1409659111, 1988.

Corte, A. and ~~A.~~ Higashi, A.: Experimental Research on Desiccation Cracks in Soil, Research Report, 66. Technical Report, Wilmette, Illinois: US Army Snow Ice and Permafrost Research Establishment, 1960.

Costa, S., ~~J. K.~~ Kodikara, ~~B.~~J. K., and Shannon, B.: Salient factors controlling desiccation cracking of clay in laboratory experiments. Géotechnique, 63, 18–29, doi:10.1680/geot.9.P.105, 2013.

~~Daniel~~Danie,l D. E. and Wu, Y. K~~. Wu,~~.: Compacted Clay Liners and Covers for Arid Sites. Journal of Geotechnical Engineering, 119(2): 223–237, doi:10.1061/(ASCE)0733-9410(1993)119:2(223), 1993.

Davarzani, H., ~~K.~~ Smits, ~~R. M.~~K., Tolene, ~~T.~~R. M., Illangasekare, T.: Study of the effect of wind speed on evaporation from soil through integrated ~~modeling~~modelling of the atmospheric boundary layer and shallow subsurface, Water Resour. Res., 50, 661–680, doi:10.1002/2013WR013952, 2014.

Dexter, A. R., Advances in characterization of soil structure. Soil and Tillage Research, 199-238, doi:10.1016/0167-1987(88)90002-5, 1988.

Dinka, T. M. and ~~R. J.~~ Lascano, R. J.: Review Paper: Challenges and Limitations in Studying the Shrink-Swell and Crack Dynamics of Vertisol Soils, Open Journal of Soil Science, 2, 82-90, doi:10.4236/ojss.2012.22012, 2012.

Everest, T. and H. Ozcan, H.: The Properties and Comparison of the Vertisol Soils Formed on Different Physiographies, International Journal of Sciences and Research, Vol. 72, No. 12, doi:10.21506/j.ponte.2016.12.12, Dec. 2016.

Fang, C. and J. B. Moncrieff, J. B.: An open-top chamber for measuring soil respiration and the influence of pressure difference on CO2 efflux measurement, Functional Ecology, 12, 319–325, doi:10.1046/j.1365-2435.1998.00189.x, 1998.

Farrell, D. A., L. E. Greacen, C. G.L. E., Gurr, C. G.: Vapor Transfer in Soil due to Air TurbulmenceTurbulence, Soil Science-Volume 102 - Issue 5 – p. 305-313, 1966.

Ferretti, D. F., E. Pendall, J.A.E., Morgan, J.A., Nelson, D.J.A., LeCain, A.R.D., and Mosier, A.R.: Partitioning evapotranspiration fluxes from a Colorado grassland using stable isotopes: Seasonal variations and ecosystem implications of elevated atmospheric CO2, Plant and Soil, 254: 291–303, doi:10.1023/A:1025511618571, 2003.

Fredlund, D. G.,: Comparison of soil suction and one-dimensional consolidation characteristics of a highly plastic clay. M.Sc., thesis, University of Alberta, Edmonton, doi:10.4224/20378888, 1964.

Fukuda, H.,: Air and water Vapor movement in soil due to wind gustiness, Soil Sci., vol 79 (249-258), 1955.

Geistlinger, H. and F. Leuther, F.: Evaporation Study for real soils based on HYPROP hydraulic functions and micro-CT measured pore-size distribution. Vadose Zone J., 17:180041, doi:10.2136/vzj2018.02.0041, 2018.

Good, S. P., D. Noone, G.D., and Bowen, G.: Hydrologic connectivity constrains partitioning of global terrestrial water fluxes, Science, 10 Vol. 349, Issue 6244, pp. 175-177, doi:10.1126/science.aaa5931, 2015.

Goulden, M.L., J.W. Munger, S-M.J.W., Fan, B.C.S-M., Daube, SB.C., and Wofsy, S.C.: Measurements of carbon sequestration by long-term eddy covariance: methods and a critical evaluation of accuracy. Glob. Change Biol., 2, 169–182, doi:10.1111/j.1365-2486.1996.tb00070.x, 1996.

Hanks, R. J. and N. P. Woodruff, N. P.: Influence of Water Vapor Transfer Trough Soil, Gravel, and Straw Mulches, Soil Science, Vol. 86, No. 3, 160–164, doi:10.1097/00010694-195809000-00010, 1958.

Hao, X. M., C. Li, B.C., Guo, J. X.B., Ma, M.J. X., Ayup, Z. S.M., qand Chen, Z. S.: Dew formation and its long-term trend in a desert riparian forest ecosystem on the eastern edge of the Taklimakan Desert in China. J. Hydrol., 472–473, 90–98, doi:10.1016/j.jhydrol.2012.09.015, 2012.

Harris, F. S.,: Factors Affecting the Evaporation of Moisture from the Soil, Journal of Agricultural Research, Vol. VII, No. 10 Dec.4, 1916.

Hatano, R., H. Nakamoto, T.H., Sakuma, H.T., and Okajima, H.: Evapotranspiration in cracked clay field soil, Soil Science and Plant Nutrition, 34:4, 547-555, doi:10.1080/00380768.1988.10416470, 1988.

Heinemeyer, A., C. Di Bene, A.R.C., Lloyd, D.A.R., Tortorella, R.D., Baxter, B.R., Huntley, A.B., Gelsomino, A., and P. Ineson, P.: Soil respiration: implications of the plant-soil continuum and respiration chamber collar-insertion depth on measurement and modelling of soil CO_2 efflux rates in three ecosystems, European journal of soil science 62 (1), 82-94, doi:10.1111/j.1365-2389.2010.01331.x, 2011.

Hill, R. J.: Implications of Monin–Obukhov Similarity Theory for Scalar Quantities, Journal of Atmospheric Sciences, 46(14), 2236-2244, doi:10.1175/1520-0469(1989)046<2236:IOMSTF>2.0.CO;2, 1989.

Hillel, D.,: Introduction to Environmental Soil Physics. Elsevier Academic Press, Amsterdam, doi:10.1016/B978-0-12-348655-4.X5000-X, 2004.

Heitman, J. L., X. Xiao, R.X., Horton, R., and T. J. Sauer, T. J.: Sensible heat measurements indicating depth and magnitude of subsurface soil water evaporation. Water Resources Research, 44, W00D05. doi.org:10.1029/2008WR006961, 2008.

Heitman, J. L., X. Zhang, X.., Xiao, T.X., Ren, T., and R. Horton, R.: Advances in heat-pulse methods: Measuring soil water evaporation with sensible heat balance. Methods of Soil Analysis, 2(1), doi.org:10.2136/msa2015.0029, 2017.

Hollinger, D.Y., S.M. Goltz, E.A.S. M., Davidson, J.T.E. A., Lee, K.J. T., Tu, H.T.K., and Valentine, H.T.: Seasonal patterns and environmental control of carbon dioxide and water vapor exchange in an ecotonal boreal forest. Glob. Change Biol., 5, 891–902, doi:10.1046/j.1365-2486.1999.00281.x, 1999.

Holmes, R. M.,.: Estimation of soil moisture content using evaporation data. Proceedings of Hydrology Symposium, No. 2 Evaporation. Queen's Printer, Ottawa, 184-196, 1961.

Jabro Jay D.,: Water Vapor Diffusion Through Soil as Affected by Temperature and Aggregate Size, Transp. Porous Med., 77:417–428, doi:10.1007/s11242-008-9267-z, 2009.

Janssens, I.A., A.S. Kowalski, B.A.S., Longdoz, R.B., and Ceulemans, R.: Assessing Forest soil CO2 efflux: an in-situ comparison of four techniques. Tree Phys., 20, 23–32, doi:10.1093/treephys/20.1.23, 2000.

Johansen, R. T. and Dunning, H. N.,: Water-vapor adsorption on clays, Clays and Clay Miner., 6(1):249–258, 1957.

Kimball, B. A. and E. R. Lemon, E. R.: Spectra of Air Pressure Fluctuation at the Soil Surface, Journal of Geophysical Research, VOL. 75, No. 33, doi: 10.1029/JC075i033p06771, 1970.

Kimball B. A. and E. R. Lemon, E. R.: Theory of soil air movement due to pressure fluctuations, Agric. Meteorol., 9 163-181, doi: 10.1016/0002-1571(71)90020-3, 1971.

Kimball, B. A., K. J. Boote, K. J. L., Hatfield, J. L. R., Ahuja, C.L. R., Stockle, S.C., Archontoulis, C.S., Baron, B.C., Basso, P.B., Bertuzzi, J.P., Constantin, D.J., Deryng, B.D., Dumont, J L.B., Durand, F.J-L., Ewert, T.F., Gaiser, S.T., Gayler, M. P.S., Hoffmann, Q.M. P., Jiang, S H.Q., Kim, J.S-H., Lizaso, J. S., Moulin, C. Nendel, C. P., Parker, T. Palosuo, E.T., Priesack, Z.E., Qi, A.Z., Srivastava, T.A., Stella, F.T., Tao, K. R.F., Thorp, D.K. R., Timlin, T. E.D., Twine, H.T. E., Webber, M.H., Willaume, K.M., and Williams, K.: Simulation of maize evapotranspiration: An inter-comparison among 29 maize models, Agricultural and Forest Meteorology, 271, 264–284, doi:10.1016/j.agrformet.2019.02.037, 2019.

Kodikara, J. K., S. L. Barbour, D. G.S. L., and Fredlund, D. G.: Desiccation cracking of soil layers. In Proceedings of the Asian Conference on Unsaturated Soils, UNSAT-Asia, Singapore (pp. 693–698). Balkema., 2000.

Kodikara, J, S. L. K., Barbour, D.G.S. L., and Fredlund, D.G.: Structure development in surficial heavy clay soils: A synthesis of mechanisms. Australian Geomechnics, 37(3): 25–40, 2002.

Koola, D., N. Agam, N.., Lazarovitch, J.L.N., Heitman, T.J. L., Sauer, A.T. J., and Ben-Gal, A.: A review of approaches for evapotranspiration partitioning, Agricultural and Forest Meteorology, 184, 56– 70, doi:10.1016/j.agrformet.2013.09.003, 2014.

Kurtzman, D., S. Baram, O.S., and Dahan, O.: Soil–aquifer phenomena affecting groundwater under vertisols: a review, Hydrol. Earth Syst. Sci., 20, 1–12, doi:10.5194/hess-20-1-2016, 2016.

Kustas, W. P., N., and Agam, N.: Soil Evaporation, Encyclopedia of Natural Resources, doi:10.1081/E-ENRL-120049129, 2014

Lai D. Y. F., N. T. Roulet, E. R.N. T., Humphreys, T .E. R., Moore, M.T. R., and Dalva, M.: The effect of atmospheric turbulence and chamber deployment period on autochamber CO_2 and CH_4 flux measurements in an ombrotrophic peatland, Biogeosciences, 9, 3305–3322, doi:10.5194/bg-9-3305-2012, 2012.

Law, B.E., D.D. Baldocchi, P.M. Anthoni, Belowcanopy and soil CO2 fluxes in a ponderosa pine forest. Agric. For. Meteorol., 94, 171–188, doi:10.1016/s0168-1923(99)00019-2, 1999.

Le Dantec, V., D. Epron, E.D. and Dufrênen, E.: Soil CO2 efflux in a beech forest: comparison of two closed dynamic systems, Plant and Soil, 214: 125–132, 1999.

Leelamanie, D.A.L.,.: Changes in Soil Water Content with Ambient Relative Humidity in Relation to the Organic Matter and Clay, Tropical Agricultural Research & Extension, 13(1), doi:10.4038/tare.v13i1.3130, 2010.

Likos, W. J. and N. Lu, N.: Water vapor sorption behavior of smectite-kaolinite mixtures, Clays and Clay Miner., 50(5), doiI:10.1346/000986002320679297, 2002.

Longdoz, B., M. Yernaux, M., and Aubinet, M.: Soil CO2 efflux measurements in a mixed forest: impact of chamber disturbances, spatial variability and seasonal evolution, Global Change Biology, 6, 907-917, doi:10.1046/j.1365-2486.2000.00369.x, 2000.

Lau, J. T. K.,.: Desiccation cracking of clay soils. MSc Thesis, Department of Civil Engineering, University of Saskatchewan, Canada https://harvest.usask.ca/handle/10388/etd-03242010-112414, 1987.

Maier, M., M. Aubinet, B.M., Longdoz, F.B., and Parent, F.: Turbulence Effect on Gas Transport in Three Contrasting Forest Soils, Soil Sci. Soc. Am. J., doi:10.2136/sssaj2011.0376, 2011.

Mohr, M., T. Laemmel, M.T., Maier, D.M., and Schindler, D.: Gas Concentrations within a Scots Pine Forest Atmosphere, 7, 125; doi:10.3390/atmos7100125, 2016.

Mohr, M., T. Laemmel, M.T., Maier, D.M., and Schindler, D.: Spatial variability of wind-induced air pressure fluctuations responsible for pressure pumping, Tellus B.,.: 69, 1361757, doi:10.1080/16000889.2017.1361757, 2017.

Morris, P. H., Graham, J., and Williams, D. J..: Cracking in drying soils. Canadian Geotechnical Journal, 29, 263–277, doi:10.1139/t92-030, 1992.

Myklebust, M. C., L.E. Hipps, L. E., and R.J. Ryel, R. J.: Comparison of eddy covariance, chamber, and gradient methods of measuring soil CO_2 efflux in an annual semi-arid grass, Bromus tectorum. Agricultural and Forest Meteorology, 148(11), 1894–1907, doi:10.1016/j.agrformet.2008.06.016, 2008.

Nachshon U., M. Dragila, N.M., and Weisbrod, N.: From atmospheric winds to fracture ventilation: Cause and effect, J. Geophys. Res., 117, G02016, doi:10.1029/2011JG001898, 2012.

Nahlawi, H. and J. K. Kodikara, J. K.: Geotech Geol Eng, 24: 1641. doi:10.1007/s10706-005-4894-4, 2006.

Nakano T., T. Sawamoto, T., Morishita, G.T., Inoue, R.G., and Hatano, R.: A comparison of regression methods for estimating soil–atmosphere diffusion gas fluxes by a closed-chamber technique, Soil Biology and Biochemistry, Volume 36, Issue 1, January, Pages 107-113, doi:10.1016/j.soilbio.2003.07.005, 2004.

Norman, J. M., C.J. Kucharik, S.T.C. J., Gower, D.D.S. T., Baldocchi, P.M.D. D., Crill, P. M., Rayment, K.M., Savage, R.G.K., and Striegl, R. G.: A comparison of six methods for measuring soil-surface carbon dioxide fluxes. J. Geophys. Res., 102, 28771–28777, doi:10.1029/97JD01440, 1997.

Oki, T and S. Kanae, S.: Global hydrological cycles and world water resources, Science, 313:1068–1072, doi:10.1126/science.1128845, 2006.

Pal, D. K., T. Bhattacharyya, T., and Suhas P. Wani, S. P.: Formation and Management of Cracking Clay Soils (Vertisols) to Enhance Crop Productivity Indian Experience January 2012, World Soil resources and Food Security Chapter 7, CRC Press, Rattan Lal and B. A. Stewart, 2012.

Pavelka, M, P., Sedlák, M.P., Acosta, R.M., Czerný, K.R., Taufarová, K., and D. Janouš, D.: Chamber techniques versus eddy covariance method during nighttime measurements, International Scientific Conference, Slovakia, Střelcová, K., Škvarenina, J. & Blaženec, M. (eds.), 2007.

Pavelka, M., M. Acosta, R.M., Kiese, N.R., Altimir, C.N., Brümmer, P.C., Crill, E.P., Darenova, R.E., Fuß, B.R., Gielen, A.B., Graf, L.A., Klemedtsson, A.L., Lohila, B.A., Longdoz, A.B., Lindroth, M.A., Nilsson, S. M., Jiménez, L.S. M., Merbold, L., Montagnani, M.L., Peichl, M., Pihlatie, J.M., Pumpanen, P. S.J., Ortiz, H.P. S., Silvennoinen, U.H., Skiba, P.U., Vestin, P., Weslien, D.P., Janous, D., and W. Kutsch, W.: Standardisation of chamber technique for CO_2, N_2O and CH_4 fluxes measurements from terrestrial ecosystems, Int. Agrophys, 32, 569-587, doi:10.1515/intag-2017-0045, 2018.

Péron, H., L. Laloui, T.L., and Hueckel, T.: Experimental evidence in desiccation cracking, Advanced Experimental Unsaturated Soil Mechanics, Proceedings of Conference, Trento, Italy, April 2005, 475–480, doi:10.1061/40802(189)87

Philip J. R.,: Evaporation, and Moisture and Heat Fields in the Soil, Journal of Atmospheric Sciences, vol. 14, Issue 4, pp.354-366, doi:10.1175/1520-0469(1957)014<0354:EAMAHF>2.0.CO;2, 1957.

Pilgrim, D. H., T. G., Chapman, DT. G., Doran, D. G., Problems of rainfallrunoff modelling in arid and semiarid regions/Problèmes de la mise au point de modèles pluie-écoulement dans les 15 régions arides et semi-arides, Hydrolog. Sci. J. (1988), 33, 379–400

Poulsen, T. G., A. Pourber, A., Furman, K.A., and Papadikis, K.: Relating wind-induced gas exchange to near-surface wind speed characteristics in porous media. Vadose Zone J., 16(8), doi:10.2136/vzj2017.02.0039, 2017.

Pourbakhtiar, A., T. G. Poulsen, S.T. G., Wilkinson S., and J. W. Bridge, J. W.: Effect of wind turbulence on gas transport in porous media: experimental method and preliminary results, European Journal of Soil Science, 68, 48–56, doi: 10.1111/ejss.12403, 2017

Risk, D., N. Nickerson, N., C. Creelman, G. McArthur, J.G., and Owens, J.: Forced Diffusion soil flux: A new technique for continuous monitoring of soil gas efflux, Agricultural and Forest Meteorology, vol. 151, issue 12, pp. 1622-1631, doi:10.1016/j.agrformet.2011.06.020, 2001.

Riou, C.: Evaporation du sol nu et répartition des pluies - Relations établies en Tunisie à partir des résultats des cases lysimétriques. Annales de l'INRAT, vol. 50, Fasc.4, INRAT, Tunisie, 24, Also published in Cahiers de l'ORSTOM, Sér. Hydrol., vol. XIV, no. 3, 285–295, https://horizon.documentation.ird.fr/exl-doc/pleins_textes/pleins_textes_4/hydrologie/16730.pdf, 1977.

Rochette, P., B. Ellert, E. G.B., Gregorich, R. L.E. G., Desjardins, E.R. L., Pattey, R.E., Lessard, R., and B. G. Johnson, B. G.: Description of a dynamic closed chamber for measuring soil respiration and its comparison with other techniques, Can. J. Soil. Sci., 77: 195-203, 1997

Rochette, P. and G. L. Hutchinson, G. L: Measurement of Soil Respiration in situ: Chamber Techniques, Publications from USDA-ARS / UNL Faculty. 1379, https://digitalcommons.unl.edu/usdaarsfacpub/1379, 2005.

Roland, M., S. Vicca, M.S., Bahn, T.M., Ladreiter-Knauss, M.T., Schmitt, I. A.M., and Janssens, I. A.: Importance of nondiffusive transport for soil CO_2 efflux in a temperate mountain grassland, J. Geophys. Res. Biogeosci. (2015), 120, 502–512, doi:10.1002/2014JG002788.

Sánchez-Cañete, E.P., C. Oyonarte, P.C., Serrano-Ortiz, J.P., Curiel Yuste, O.J., Pérez-Priego, F.O., Domingo, A. S.F., and Kowalski (2016),A. S: Winds induce CO_2 exchange with the atmosphere and vadose zone transport in a karstic ecosystem, J. Geophys. Res. Biogeosciences, 121, doi:10.1002/2016JG003500, 2016.

Satar, E., Tes. A. Berhanu, D.T. A., Brunner, S.D., Henne, S., and M. Leuenberger, M.: Continuous CO2/CH4/CO measurements (2012–2014) at Beromünster tall tower station in Switzerland, Biogeosciences, 13, 2623–2635, doi:10.5194/bg-13-2623-2016, 2016

Sauer T. J., T. E. Ochsner, T. E., and R. Horton, R.: Soil heat flux plates: Heat flow distortion and thermal contact resistance. Agronomy Journal, 99(1), 304–310, doi.org:10.2134/agronj2005.0038s, 2007.

Schneider J., L. Kutzbach, S.L., Schulz, S., and M. Wilmking, M.: Overestimation of CO_2 respiration fluxes by the closed chamber method in low-turbulence nighttime conditions, J. Geophys. Res., 114, G03005, doi:10.1029/2008JG000909, 2009.

Schrier-Uijl, A. P., P. S. Kroon, A.P. S., Hensen, P. A., Leffelaar, F.P. A., Berendse, E. M.F., and Veenendaal, E. M.: Comparison of chamber and eddy covariance-based CO2 and CH4 emission estimates in a heterogeneous grass ecosystem on peat, Agricultural and Forest Meteorology, 150(6):825-831, doi:10.1016/j.agrformet.2009.11.007, 2010.

Scotter, D. R. and Raats, P. A. C. Raats,.: Dispersion of water vapor in soil due to air turbulence, Soil Sci., Vol. 108, No. 8 170-176,

Schmidt, G. A., R. A. Ruedy, R. L.A., Miller andA. A., R. L., and Lacis, A. A.: Attribution of the present-day total greenhouse effect, J. Geophys. Res. 2010 15 D20106, doi:10.1029/2010JD014287, 1968.

Smits, K., V. Eagen, A.V., and Trautz, A.: Exploring the Effects of Atmospheric Forcings on Evaporation: Experimental Integration of the Atmospheric Boundary Layer and Shallow Subsurface. J. Vis. Exp., 100, e52704, doi:10.3791/52704, 2015

Stirling, R. A., S. Glendinning, C.T.S., and Davie, C. T.: Modelling the deterioration of the near surface caused by drying induced cracking, Applied Clay Science, 146 176–185, doi:10.1016/j.clay.2017.06.003, 2017.

Suleau, M., A. Debacq, V.A., Dehaes, M.V., and Aubinet, M.: Wind velocity perturbation of soil respiration measurements using closed dynamic chambers, European Journal of Soil Science, 60(4):515 - 524, doi:10.1111/j.1365-2389.2009.01141.x, 2009.

Suleman, K. F., A. and Shahid, A.: Determination of the desiccation behavior of clay slurries, International Journal of Mining Science and Technology, 27 981–988, doi:10.1016/j.ijmst.2017.06.010, 2017.

Takle, E. S., W. J. Massman, W. J. R., Brandle, J. R. A., Schmidt, X.R. A., Zhou, I. V.X., Litvina, R.I. V., Garcia, G.R., Doyle, C. W.G., and Rice, C. W.: Influence of high-frequency ambient pressure pumping on carbon dioxide efflux from soil, Agricultural and Forest Meteorology, 124, Issues 3–4, 193-206, doi:10.1016/j.agrformet.2004.01.014, 2004.

Tang, C. S., B. Shi, C.B., Liu, L.C., Zhao, B.L., and Wang, B.: Influencing factors of geometrical structure of surface shrinkage cracks in clayey soils. Engineering Geology, 101, 204–217, doi:10.1016/j.enggeo.2008.05.005, 2008.

Tang, C. S., Y. J. Cui, A. M.Y. J., Tang, B.A. M., and Shi, B.: Experiment evidence on the temperature dependence of desiccation cracking behavior of clayey soils. Engineering Geology, 114, 261–266, doi:10.1016/j.enggeo.2010.05.003, 2010.

Thornthwaite, C. W. and B. Holzman, B.: Measurement of Evaporation from Land and Water Surfaces, U.S. Dept. of Agri. Tech. Bull., 817, 143, 1942.

Trenberth, K. E., J. Fasullo, J., Kiehl, J.: Earth's global energy budget. Bull. Am. Meteorol. Soc., 90:311–323, doi:10.1175/2008BAMS2634.1, 2009.

Wagner, W. and A. Pruß, A.: The IAPWS Formulation 1995 for the Thermodynamic Properties of Ordinary Water Substance for General and Scientific Use, Journal of Physical and Chemical Reference Data, June 2002, Volume 31, Issue 2, pp. 387535, doi:10.1063/1.1461829, 2002.

Wang, X.,: Vapor Flow Resistance of Dry Soil Layer to Soil Water Evaporation in Arid Environment: An Overview, Water, 7, 4552-4574 doi:10.3390/w7084552, 2015.

Wilcox, B., M. Seyfried, D.M., Breshears, D.: The water balance on rangelands, Encyclopedia of water science, 791–794, doi:710.1081/E-EWS-120010097, 2003.

Wilson, G. W., D.G. Fredlund, S.L.D. G., Barbour, S. L.: Coupled soil-atmosphere modelling for soil evaporation. Canadian Geotechnical Journal, 31(2): 151-161, doi:10.1139/t94-021, 1994.

Wilson: G. W., D.G. Fredlund, S. L.D. G., and Barbour, S. L.: The effect of soil suction on evaporative fluxes from soil surfaces, Canadian Geotechnical Journal, 34(1):145-155, doi:10.1139/cgj-34-1-145, 1997.

World Meteorological Organization WMO168 Ed 2008 Vol I Ch4 Evaporation, Evapotranspiration and Soil Moisture.

Xu, L., M.D. Furtaw, R.A.M. D., Madsen, R.L. A.,, Garcia, D.J.R. L, Anderson, D. J., and D.K. McDermitt, D. K.: On maintaining pressure equilibrium between a soil CO2 flux chamber and the ambient air, J. Geophys. Res., 111, D08S10, doi:10.1029/2005JD006435, 2006.

Zha, T., Niinisto, S., Xing, Z., Wang, K. Y., Kellomäki, S., Barrand Bar,r A. G.,: Total and component carbon fluxes of a Scots pine ecosystem from chamber measurements and eddy covariance, Ann Bot., 99(2), 45-53, doi:10.1093/aob/mcl266, 2007.

Appendix A: Laboratory measured soil evaporation *RE*

The calibration process requires extensive and comprehensive real soil evaporation measurements. Preceding *RE* measurement data, two interesting points were remarked and are briefly reported at the margin: exponential evaporation behavior for both soils in the second evaporation stage and a common point in the clayey soil.

A.1 Real evaporation *RE* on the second stage

Soil evaporation is well known and admitted to be able to be divided into three stages. (Introduced by Philip 1959, Wilsdon et al. 1994 or Hiller 2004). Wet soil, water-saturated or near water-saturated, evaporates at a constant rate depending greatly on the wind. With progressively drying soil, a second stage appears after the so-called air entry value (AEV) and shows the smallest wind dependence. A third stage concerns very dry soils with a constant extremely low evaporation rate and was not truly observed in this study except the zero-wind sand evaporation record, which took over two months of constant monitoring. To compare measurements under different wind speeds, such as the real evaporation from sandy and clayey soils, a semilogarithmic scale versus soil moisture is probably the most relevant method (Fig. A1). In these figures, we can notice that regarding the sand, the first stage is important compared to the clayey soil, where the evaporation quickly falls to the second stage. This behavior is characteristic of relatively low-rate evaporation on sandy soil (Holmes 1961). The second stage displays a very linear behavior for the sand and for the clayey soil on the logarithmic scale: in the second stage, the evaporation rate is an exponential function of the soil moisture *w*.

$$RE_{Second\ Stage} = C(w_s) * e^{D*w} \quad \text{(A1)}$$

where C depends slightly on the wind speed, and *D* is a constant almost independent of the wind speed for sandy soil. Indeed, regarding sandy soil, regardless of the wind, the slopes are the same, and the curves are parallel but remain slightly wind-affected since they are not superimposed.

For the clayey soil, the second stage evaporation rates are higher for the higher wind. There is a visible common point where the evaporation rates are the same regardless of the wind. For a lower moisture, the curves clearly diverge as the slopes are different. The common point existence is discussed in the next section.

The difference between sandy soil and clayey soil drying processes is certainly affected by the micro- and later macrodesiccation crack appearances in clayey soils (Lau 1987, Morris et al. 1992, Kodikara 2002). These cracks may be

considered an effective soil/air interface surface increase and then an additive water vapor exchange surface that may significantly increase the evaporation rate under wind (Nachshon et al. 2012). Another difference between these soils is the grain size difference and then intergrain void space and the resulting matrix suction amplitude, as discussed later in this paper.

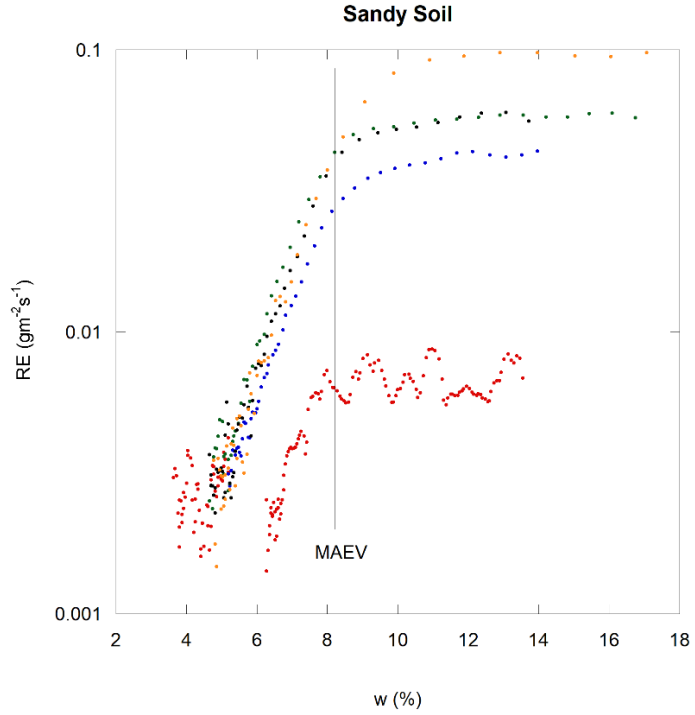
Sandy Soil
0.1
0.01
0.001
RE (gm-2s-1)
MAEV
2
4
6
8
10
12
14
16
18
w (%)

(a)

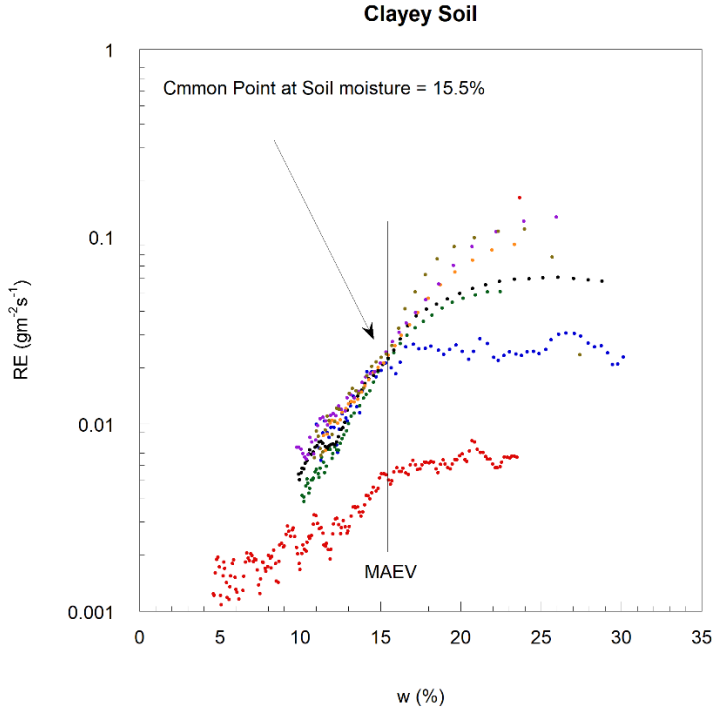
Clayey Soil
Cmmon Point at Soil moisture = 15.5%
1
0.1
0.01
0.001
RE (gm-2s-1)
MAEV
0
5
10
15
20
25
30
35
w (%)

(b)

Figure A1: Real evaporation versus gravimetric soil moisture a) for sandy soil and b) for clayey soil at several wind speeds.

A.2 Clayey soil cracking and common point.

Crack formation in drying clayey soil, also called desiccation soil cracks, has a great influence on the total evaporation up to 50% enhancement according to Hatano et al. (1988), and under windy conditions, the total evaporation may even be increased by two orders of magnitude (Nachshon et al. 2012). This phenomenon is widely studied and relatively well documented, as its consequences for engineering (Lytton et al. 1976; Daniel et al. 1993; Kodikara et al. 2002; Rodriguez et al. 2007; Stirling et al. 2017) and agriculture (Pal et al. 2012; Kurtzman et al. 2016) are very important. Figure A2 shows the clayey soil sample in its dry state; (a) dried under a moderate wind, (b) dried under no wind. During this study, different crack patterns were obtained with different wind speeds and drying ratios. An obvious wind importance effect on the cracking pattern was noticed. The cracks are more numerous with higher wind in accordance with existing studies (Corte and Higashi, 1960; Tang et al. 2008 and 2010; Costa et al. 2013), and the coarsest cracks are always in accordance with previous studies (Corte and Higashi, 1960; Lau, 1987; Kodikara et al. 2000; Nahlawi and Kodikara, 2006; Tang et al. 2008 and 2010; Costa et al. 2013) due to an important matrix suction increase with the drying ratio in clayey soil. This is a part of so-called *dynamic effects*. The studied clayey soil sample can lose up to 15% of its initial volume, and its observation drying under different wind speeds allows us to point out an interesting finding, which is the existence of a common point (*CP*) and a change in the evaporation ratio versus soil moisture slope below this point under all wind speeds but nil. The clayey soil sample cracks under wind but drying as a whole block, almost without cracks, under calm conditions (Fig. A1(b)), creating a void space between the soil block and the bucket wall.

CP corresponds to a well-defined *RE* of approximately 0.024 $gm^{-2}s$ at a soil moisture *w* of approximately 15.5%. *CP* also corresponds to the *RE* versus *w* slope change for drying soil. At the current research advancement point, one can only propose a hypothesis to explain this phenomenon tied with the clayey soil matrix air entry value (MAEV) corresponding to air seepage through the soil matrix, but the present study does not allow us to prove it. Soil *RE* slows down as the soil moisture decreases; however, in the swelling clayey soil case, the soil moisture decreases cause microcracks and hollow formation, depending on the expansive clay content (smectite minerals, including montmorillonite and bentonite) and, more precisely, its vertisol character (Ahamad 1996; Everest et al. 2016), increasing the effective soil/atmosphere interaction surface (Bronswijk 1988). This fact agrees with a relatively less pronounced transition between the first and second stages of evaporation observed in clayey soil versus sandy soil (Fig. A1). As the importance of the wind influence on the *RE* goes together with the interaction surface, any change in the latter is visible in the former. Crack formation in the soil would increase *RE by* changing the *RE* versus *w* ratio and may then explain the apparent slope change observed in Fig. A1 (b). However, the cracks transform the soil sample to a fractured medium and are visible well before the *CP* point, as shown by Song et al. (2016). Cracking forms a so-

called cracking air entry value (*CAEV*) on the moistest, almost saturated, clayey soil, and their formation is progressive, which is rather incompatible with a brusque slope change. The concerned soil moisture point *CP* seems to correspond rather to a soil matrix air entry value (Azam et al. 2013) below which the soil acts as a porous medium. The crack formation causing the first *AEV* (*CAEV*) on a soil moisture characteristic curve is followed by the matrix *AEV* (MAEV) formation on a drier soil and is very similar to a bimodal grain-size distribution curve (Satyanaga et al. 2013), where grains of both large and small sizes are present in the soil with then two intergrain void space sizes. These two points, cracks and matrix *AEV*, occur in a drying clayey under the wind before the final void ratio stabilization (Péron and Laloui 2005) and affect an evaporation ratio that is one order of magnitude larger than theorder of magnitude of no wind evaporation. Since, under no wind, the *CP* is not visible, one can deduce that cracks and/or wind presence are necessary

.

(a)

1365

(b)

Figure A2: Dried clayey soil surface after drying under (a) moderate wind of 0.8 ms^{-1}, and (b) no wind.

Appendix B: Slow sensor simulation

The response of a slow sensor to step-like variations in physical variable S is usually very close to an exponential rise evolution between the initial value M_0 and the final value M_f and characterized by the characteristic time τ_m(see Eq. 3). If the measured variable also follows a known exponential law (characteristic time τ_s, to simulate the slow sensor-provided signal), one can proceed by discretization dividing the considered time interval into several equal short intervals Δt. For example, if the considered physical variable evolution takes 100 s, we can start a simulation working with $\Delta t = 1\ s$.

Then, for each interval, we can calculate the real signal amplitude:

$$S_i = Ae^{-t_i/\tau_s} + B \tag{B1}$$

In equilibrium at the beginning, $M_0 = S_0$, the sensor will follow the real signal S evolutions with some delay deforming it. For each time interval, we can approximate its measurement evolution as an exponential rise evolution between the last reached state and a new state.

$$M_i = S_i - (S_i - M_{i-1})e^{-\Delta t/\tau_m}. \tag{B2}$$

As the results are dependent on Δt magnitude, this interval can be made increasingly smaller, for example, dividing it by 2 each time. With progressively smaller intervals Δt, each simulation will give results that became stable and do not change notably. At this time, we can consider the results accurate.

Figure B1 shows a simulation of a slow sensor ($\tau_m = 10s$) that measures an exponential rise-like signal ($\tau_s = 30s$) fitted by an exponential rise adjustment. The insert represents a zoom of the initial variations. The calculated fluxes are the product of the variation amplitude (asymptotic level less initial level) by the initial slope. The fit of slow sensor measurements has a lower slope, but the adjustment optimization process tends to overestimate the variation amplitude. There is a local maximum of that product. That is, a moderately slow sensor may lead to an overestimation of the flux.

In Fig. B1, we can see the three intersections between the measured signal and the fit, which are used to settle the second fitted interval, as shown in Fig. 02.

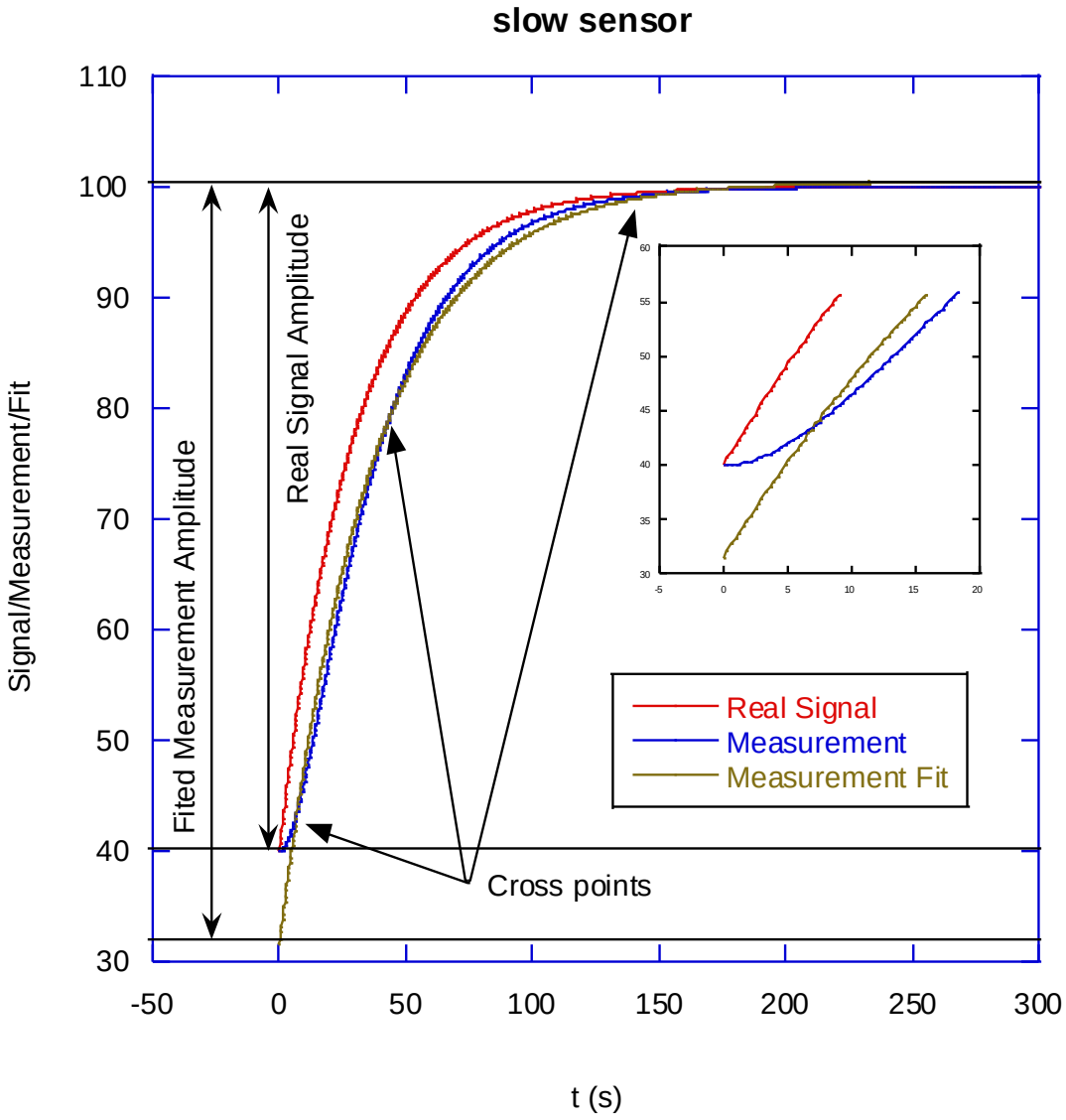

Figure B1: Real exponential rise-like signal, simulated slow sensor measurements and exponential rise fit of the measurements. Insert depicts the zoom of the initial variations.